



## RESEARCH ARTICLE

WILEY

# An assessment of future climatic and anthropogenic impacts on the hydrological system of a semi-arid catchment

Rajesh Nune<sup>1,2</sup>  | Andrew W. Western<sup>1</sup> | Biju A. George<sup>1</sup> |  
Sridhar Gummadi<sup>3</sup> | Srinivas Pasupuleti<sup>4</sup> | Ragab Ragab<sup>5</sup>  | Sreenath Dixit<sup>2</sup>

<sup>1</sup>Department of Infrastructure Engineering, Melbourne School of Engineering, University of Melbourne, Victoria, Australia

<sup>2</sup>International Crops Research Institute for the Semi-Arid Tropics, Patancheru, Hyderabad, Telangana, India

<sup>3</sup>International Center for Biosaline Agriculture (ICBA), Dubai, United Arab Emirates

<sup>4</sup>Department of Civil Engineering, IIT-ISM, Dhanbad, Jharkhand, India

<sup>5</sup>UK Centre for Ecology and Hydrology, UKCEH, Wallingford, Oxfordshire, UK

**Correspondence**

Rajesh Nune, Department of Infrastructure Engineering, Melbourne School of Engineering, University of Melbourne, Victoria 3010 Australia.  
Email: [rajeshnune@gmail.com](mailto:rajeshnune@gmail.com)

**Abstract**

Climate and catchment characteristics, particularly land and water use and management, may vary according to the population growth rate, future food habits and water demands. Three climate simulations corresponding to the Intergovernmental Panel on Climate Change, Special Report on Emissions Scenarios (A1B) were downscaled using the 'Providing Regional Climates for Impact Studies' (PRECIS) for the period 1961–2098, and bias correction was performed using the quantile mapping (QM) method. A semi-distributed integrated model (Modified Soil and Water Assessment Tool, SWAT) was used to predict the impacts of dynamic changes in catchment characteristics in the Himayat Sagar (HS) catchment and the effects of future climate change on future streamflow and groundwater storage. Simulations predicted that if this trend continues in the future, future climate and anthropogenic changes will lead to a more than 50% reduction in streamflow and a 50% increase in actual evaporation in the HS catchment. This would reduce groundwater storage to a depth of 15 m compared to current conditions, and by the end of the century, there would be no contribution from the base flow to the streamflow. Overall, unless current policies are modified to stabilize land and water management practices, anthropogenic changes will have greater importance than climate change.

**KEYWORDS**

anthropogenic changes, climate change, groundwater extraction, irrigation expansion, streamflow changes and groundwater exploitation

**Résumé**

Les caractéristiques du climat et du bassin versant, en particulier l'utilisation et la gestion des terres et de l'eau, peuvent varier selon le taux de croissance démographique, les habitudes alimentaires futures et la demande en eau. Trois simulations climatiques correspondant au Rapport spécial sur les scénarios

Article title in French: Évaluation des impacts climatiques et anthropiques futurs sur le système hydrologique d'un bassin versant semi-aride.

This is an open access article under the terms of the [Creative Commons Attribution](https://creativecommons.org/licenses/by/4.0/) License, which permits use, distribution and reproduction in any medium, provided the original work is properly cited.

© 2024 The Author(s). *Irrigation and Drainage* published by John Wiley & Sons Ltd on behalf of International Commission for Irrigation and Drainage.

d'émissions (A1B) du Groupe d'experts intergouvernemental sur l'évolution du climat ont été diminuées à l'aide de la méthode «Providing Regional Climates for Impact Studies» (PRECIS) pour la période 1961–2098, et la correction des biais a été effectuée à l'aide de la méthode de cartographie des quantiles (QM). Un modèle intégré semi-distribué (Outil d'évaluation des sols et des ressources en eau modifié, SWAT) a été utilisé pour prédire les impacts des changements dynamiques sur les caractéristiques du bassin versant de l'Himayat Sagar (HS) et les effets des changements climatiques futurs sur le débit fluvial et le stockage des eaux souterraines. Les simulations ont prédit que si cette tendance se poursuit à l'avenir, les changements climatiques et anthropiques futurs entraîneront une réduction de plus de 50% du débit fluvial et une augmentation de 50% de l'évaporation réelle dans le bassin versant de l'Himayat Sagar. Cela réduirait le stockage des eaux souterraines à une profondeur de 15 m par rapport aux conditions actuelles et, d'ici la fin du siècle, il n'y aurait aucune contribution du débit de base au débit fluvial. Dans l'ensemble, à moins que les politiques actuelles ne soient modifiées pour stabiliser les pratiques de gestion des terres et des eaux, les changements anthropiques auront une importance très supérieure à celle des changements climatiques.

#### MOTS CLÉS

changements climatiques, changements anthropiques, prélèvement des eaux souterraines, expansion de l'irrigation, changements de débit et exploitation des eaux souterraines

## 1 | INTRODUCTION

One of the most important natural resources that has to be properly managed to meet human requirements, including food and health, is water. The availability of water resources in a hydrological system is affected over time by exogenous (caused by nature) and endogenous (induced by human activities) forces or both and will continue to be affected in the future. Endogenous forces are human actions that alter the characteristics of catchments, whereas exogenous forces are natural processes and human activities that increase greenhouse gas concentrations in the atmosphere and cause climate change (Mohammed et al., 2020; Müller & Levy, 2019; Neal et al., 2002; Padowski et al., 2015). Particularly in semi-arid areas of emerging nations, climate and catchment changes are extremely dynamic both spatially and temporally (Nune et al., 2014). These forces change the catchment's entire water balance proportion, including evapotranspiration, soil moisture, groundwater recharge, and streamflow and groundwater storage. The last few decades have seen an increase in interest in determining the various forces altering the hydrological system and evaluating the relative contributions of each force. According to recent studies, during the planning and management of water resources, both exogenous and endogenous

changes occur since they have a significant impact on watershed hydrology (Cooley et al., 2021; Marvel et al., 2019; Yang et al., 2021). An integrated surface and groundwater hydrological model can be used to assess the relative contributions of each of these forces to historical conditions. It is also possible to forecast the future effects of various forces by extrapolating their trends from government initiatives. The prediction of future hydrological changes driven by dynamic anthropogenic and climate changes can aid in the development of strategies to manage water resources in the context of future challenges.

Climate change refers to any long-term changes in the mean and/or variability of the climate in any region (IPCC, 2007 2014). There is no doubt that the global climate system is changing, especially in terms of rising temperatures, as confirmed by the IPCC Six Assessment Report (AR6) (IPCC, 2023). Through variations in precipitation intensity and frequency in addition to evapotranspiration caused by fluctuations in temperature, radiation and wind speed, climate change has a direct impact on hydrological processes. These modifications may result in changes in soil moisture availability, evapotranspiration and hydrological extremes such as peak and low flows driven by flood and drought events (Afzal & Ragab, 2019, 2020a, 2020b; Saft et al., 2015). Studies are usually conducted using the output data of a general circulation

model (GCM) downscaled with regional climate models (RCMs) to determine the influence of climate change. To understand the effects of fluctuations in temperature and precipitation on the water resources of numerous river basins worldwide, a great deal of research has been conducted (Gosling & Arnell, 2016; Haddeland et al., 2014). For instance, research has indicated that variations in precipitation and projected increases in temperature may impact not only water reserves but also aquatic and terrestrial environments across various regions of the world (Allen et al., 2010; Cristea & Burges, 2010). In the United States, streamflow into the Mono Lake basin in California is projected to decrease by 15% by the end of 2030 compared to historical levels. Furthermore, it has been noted that in many catchments, climate change is associated with an increase (7–22%) in the frequency of drought conditions and a decrease (0–15%) in the frequency of flood conditions (Ficklin et al., 2013). An analysis conducted by Chiew and McMahon, (2002) revealed how climate change might affect streamflow in Australia by 2030 in the north-east (−5% to 15%) and east coast (−15% to 15%) catchments. Apart from the projected fluctuations in streamflow in certain catchments, it has been discovered that extended drought conditions (spanning across decades) cause modifications in the relationships between rainfall and runoff in dry, flatter and less wooded catchments in south-east Australia (Saft et al., 2015). The Gediz and Buyuk Menderes sub-basins in Turkey are projected to experience 20, 35 and 50% reductions in surface water by 2030, 2050 and 2080, respectively, as a result of climate change (Ozkul, 2009). According to a study conducted in India on 12 significant river basins, streamflow will decline in the future, and the intensity of floods and droughts will increase (Gosain et al., 2006). In many parts of the world, streamflow and catchment hydrology have been significantly impacted as a result of climate change (Dingbao & Alimohammadi, 2012; Kusangaya et al., 2014; Middelkoop et al., 2001).

Endogenous catchment changes are typically anthropogenic and mostly induced by water use. Examples of this include the indiscriminate exploitation of surface and groundwater resources in catchments, as well as the expansion of irrigated areas (land use change) as a result of harvesting surface runoff through water storage structures (Alemayehu et al., 2007; Ashraf et al., 2007; Beavis et al., 1997; Callow & Smettem, 2009; Garg et al., 2012; Jordan et al., 2008; Niehoff et al., 2002; Quilbé et al., 2008; Siriwardena et al., 2006; Stone & Hansen, 2016). Such changes have been found to affect the streamflow, groundwater storage and overall water availability of catchments in many regions (Rockstrom et al., 2009; Shiklomanov, 1989, 1997; Shiklomanov et al., 2011). In particular, increased irrigated land in the Himayat Sagar

catchment (India) has led to a decrease in groundwater levels and an increase in actual evapotranspiration due to anthropogenic changes (Nune et al., 2014). Furthermore, in the Himayat Sagar basin and many other catchments, the base flow contribution to streamflow has decreased due to the overabstraction of groundwater resources (Ashraf et al., 2007; Nune et al., 2014; Schreider et al., 2002; Venkateswara Rao et al., 2006).

Future climate change and catchment changes will likely continue to jeopardize the sustainability of water supplies, which will be extremely difficult in many semi-arid regions of the world. Understanding the effects of climate change and different anthropogenic activities on watershed hydrology has been the focus of several studies conducted throughout the world. For example, there are numerous studies on how climate change affects basin agricultural productivity, streamflow and total water availability (Bouwer et al., 2006; Murugan et al., 2005). Similarly, a number of studies have examined how streamflow and water storage are affected by both human activity and climate change (Baloch et al., 2015; Mittal et al., 2016; Pohle et al., 2015; Zhang & Lu, 2009). However, the majority of these studies have focused on the impacts of climate change, catchment changes or both on streamflow or groundwater storage. Few studies have examined all of the dynamic drivers of change (caused by anthropogenic activities and climate) across all of the hydrological components of a catchment. Recently, scientific effort has shifted its focus to understanding the possible causes of change and evaluating the relative effects of anthropogenic and climate change on hydrological systems to manage current and future challenges.

Water resources must be understood at the scale at which they are managed, as management effects may vary from location to location due to heterogeneity in catchment characteristics. A common approach for studying climate and anthropogenic impacts on catchment hydrology is therefore to use hydrological models to represent the hydrological processes and climate conditions of specific catchments. The Soil and Water Assessment Tool (SWAT) (Arnold et al., 1998; Arnold & Fohrer, 2005), is a semi-distributed hydrological model that is widely used in different river basins throughout the world and was used in this study to simulate hydrological processes and address various hydrological problems. It operates continuously on a daily timescale, and SWAT is known for its high efficiency in reproducing hydroclimate systems using available climate and catchment characteristics data. The SWAT model has been applied successfully to address the impacts of climate change and human activity on water availability in various parts of the world due to its high computational efficiency (Afzal & Ragab, 2020, 2020b; Desai et al., 2020; Gosain et al., 2006; Gosling & Arnell, 2016).

For example, Ribeiro et al. (2022) examined the effects of land use and climate changes on the availability of all water resources using the SWAT model. Similarly, other studies have applied the SWAT model to analyse the impacts of climate change and human activities on river runoff and catchment evapotranspiration (Desai et al., 2020; Senent-Aparicio et al., 2018). To examine these

effects on the sustainability of river basins throughout the century, the SWAT model has also been coupled with groundwater models to simulate all horizontal and vertical fluxes, including recharge and pumping at the sub-basin level (Nune et al., 2021; Perkins & Sophocleous, 2000; Perrin et al., 2012; Zhang et al., 2020). However, only a small number of studies have examined the impacts of

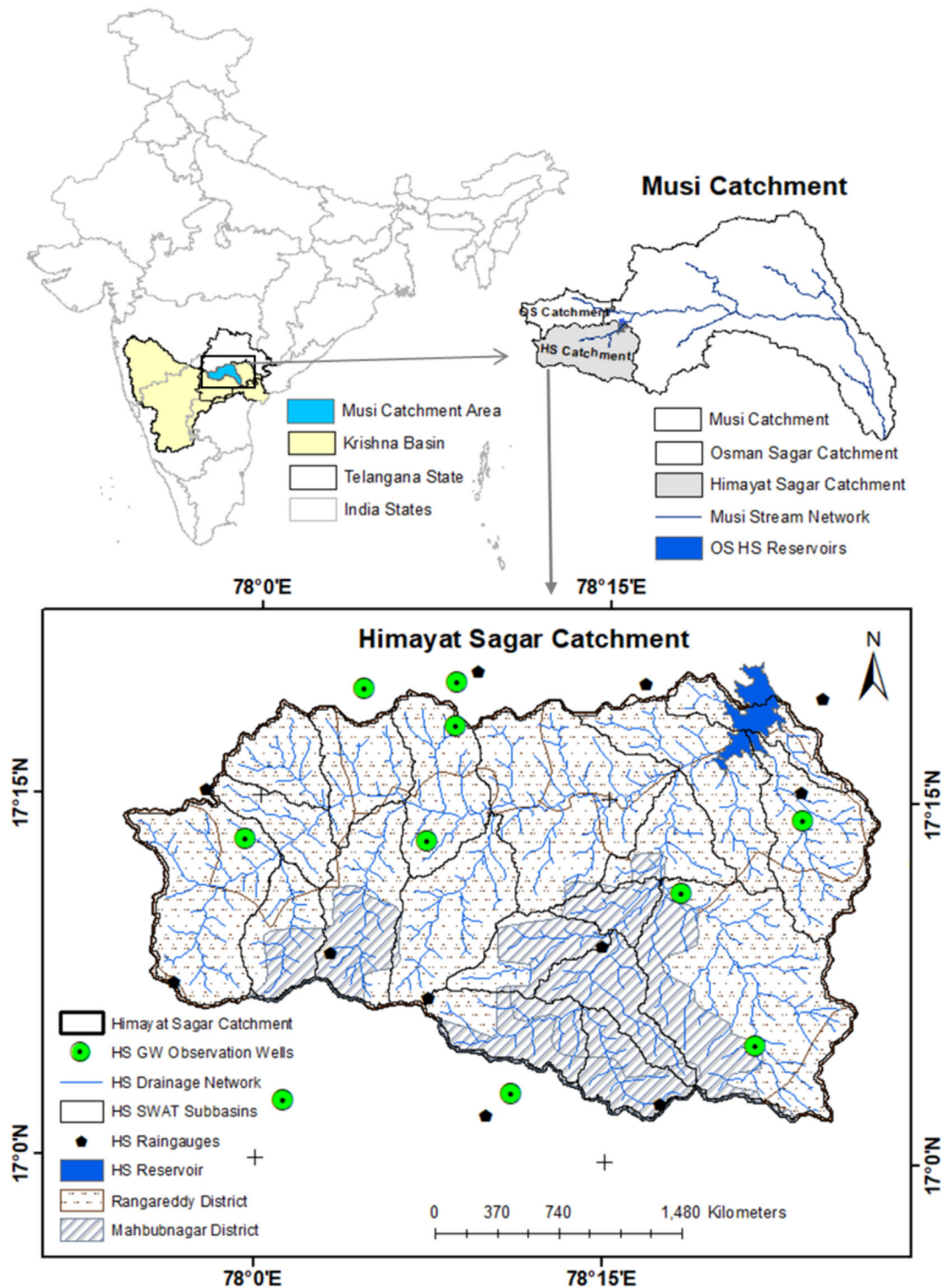


FIGURE 1 Map showing the location of the Himayat Sagar catchment in southern India.

changing climate and watershed characteristics, both spatially and temporally, on all of the hydrological processes (both vertical and horizontal fluxes) of Indian river basins.

Therefore, this study aimed to examine the potential impacts of future exogenous (climate change) and endogenous (anthropogenic activity) forces on the hydrology of a semi-arid catchment. The Himayat Sagar (HS) catchment, a subcatchment of the Musi river basin in southern India, was selected as a case study to analyse the potential impacts of future changes on catchment hydrology (Figure 1). Three climate perturbations of the PRECIS data (Q0, Q1 and Q14 of the A1B emission scenarios), which were bias corrected using the quantile mapping method, were employed in this investigation. Historical trends, such as changes in land use and water storage capacity in the HS catchment, are utilized for predicting future anthropogenic changes. To quantify the impacts of climate change and human activities on the hydrology of the HS catchment, a modified SWAT model, a coupled SWAT model with a groundwater model, was used. It was calibrated and validated against the historical flow and groundwater storage of the HS catchment (Nune et al., 2021).

This paper discusses the comprehensive assessment framework adopted to assess the potential future individual and combined impacts of climate and anthropogenic changes on streamflow and groundwater storage in the HS catchment. Specifically, it aims to:

- Examine the individual impacts of climate change by keeping catchment characteristic conditions unchanged; and
- Examine the combined impact of climate and catchment changes (both land use and water storage capacities) for the three climate perturbations.

## 2 | STUDY AREA

The Himayat Sagar (HS) catchment is one of the sub-basins of the Musi river and is located in the Krishna river basin of south India. The total geographical area of the HS catchment is 1,340 km<sup>2</sup>, as shown in Figure 1. The HS catchment receives an average annual rainfall of 718 mm, 90% of which occurs in a 4-month period (June–September) during the south-west monsoon season. The runoff generated from the catchment drains into the River Esa. In 1927, a reservoir called the Himayat Sagar reservoir was constructed on this river to control floods and supply drinking water to Hyderabad city; it is located 9.6 km upstream of that city. The overflow from the HS reservoir joins the Musi river downstream of the catchment. Temperatures in the catchment vary from 44°C in summer to 12°C in winter (George et al., 2007). The soils spread across this catchment are predominantly clay, and there are also loamy and rock formations (Gurunadha Rao et al., 2007). In this catchment, crops are grown mainly in two seasons, the *khari* season (June to November) and the *rabi* season (December to March), and agricultural lands are kept fallow during the summer period.

The HS catchment underwent many complex changes from 1980 to 2007. The net irrigated area doubled between 1980 and 2000, and as a result of a watershed development programme in the catchment, the total water-harvesting area and volume of watershed structures increased from 1 to 3 km<sup>2</sup> and from  $1.1 \times 10^6$  to  $6 \times 10^6$  m<sup>3</sup>, respectively (Nune et al., 2014, 2021). The streamflow into the HS reservoir during the study period (1980–2007) showed a declining trend, although no significant trend was observed in the average annual rainfall (Figure 2). During this period, the streamflow into the

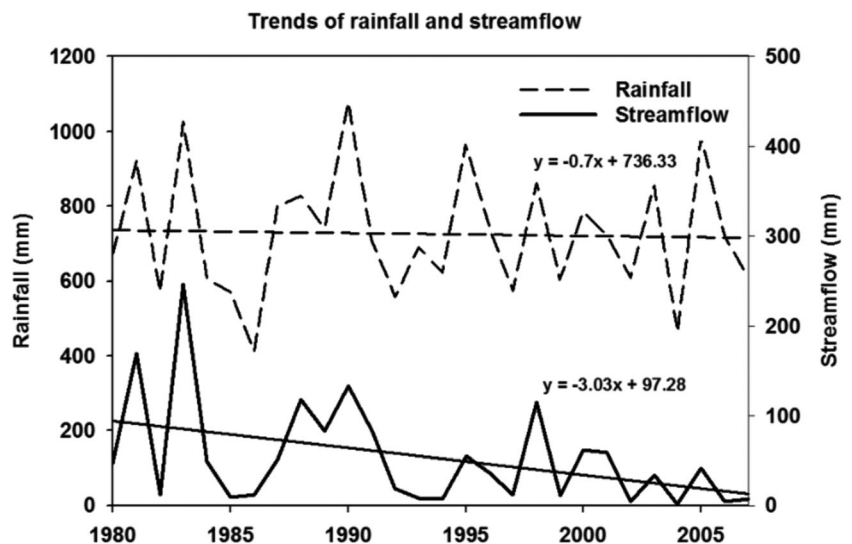


FIGURE 2 Annual rainfall and observed annual streamflow in the Himayat Sagar catchment.

HS reservoir decreased from 14% of the total rainfall (from 1980 to 1984) to less than 5% (from 2000 to 2004), and the average groundwater level decreased by approximately  $0.18 \text{ m yr}^{-1}$  (Massuel et al., 2013; Nune et al., 2014). Overall, during the study period, it was observed that the decrease in HS streamflow was mainly due to an increase in the area under irrigation but not due to increased runoff interception storage in the HS catchment (Nune et al., 2014).

### 3 | DATA AND METHODS

In this study, bias-corrected PERECIS (Providing Regional Environments for Impact Studies) climate data and future catchment change data, derived from historical observations (1980–2007), were used to analyze the impacts of these changes on the hydrology of the HS catchment (Jones et al., 2004; Rupa Kumar et al., 2006; Themebl et al., 2012). Data obtained from the relevant state government departments in Telangana state during the historical period (1980–2007) were used to model the watershed characteristics, model calibration and validation, including climate, land use, soil qualities, reservoir inflows, groundwater levels and temporal and spatial distributions of water-harvesting structures (Nune et al., 2014, 2021). The estimation of groundwater pumping rates in the watershed during the *kharif* and *rabi* seasons was derived from a direct survey of farmers and cross-checked with the literature (Perrin et al., 2012). The stage–area–volume data of different small water-harvesting structures were directly collected from the structures during field visits and for larger village water tanks, and the data were obtained through interpretation of remote sensing images (unsupervised classification) and Google Earth images of the catchment. More details of these methods (PRECIS data and quantile mapping) are explained in detail in the following sections. The impacts of future hydrological changes caused by changes in climate and watershed features are examined separately for three distinct climate periods: early century (2041–2040), middle century (2041–2070) and late century (2071–2098).

#### 3.1 | Overview of the modified SWAT model and set-up

The modified SWAT model was developed to capture trends in streamflow and groundwater storage/levels due to climatic and anthropogenic changes that occurred in the study catchment. The modified SWAT tool was developed using the MATLAB programming language, a

commercial software package that directly expresses matrix and array mathematics (The MathWorks Inc., 2012). It is an integrated model of surface and groundwater systems that operates on a daily time step. The surface, plant and soil profile processes of the model are similar to those in the SWAT model, and they estimate processes for each hydrological response unit (HRU) (Arnold et al., 1998).

The modified SWAT model differs from the SWAT model in the estimation of the recharge component. The recharge from all HRUs in a sub-basin is aggregated, which then becomes the input to the lumped groundwater storage model, which simulates groundwater processes at the sub-basin level. The modified SWAT model estimates the potential evapotranspiration using the modified FAO Penman–Monteith equation, as in the SWAT model (Allen et al., 1998). Actual evapotranspiration constitutes evaporation from soils, water bodies (watershed development structures, village water bodies and depression storages) and transpiration by vegetation. The total volume of large water storage structures (reservoirs/natural lakes/natural tanks) within a sub-basin was aggregated and represented as a reservoir at the outlet of each sub-basin. The total volume of small watershed development structures is aggregated and simulated within each HRU. Both the watershed development structures and village water bodies are spatially simulated considering their daily capacity, inflow and outflow, and seepage and evaporation. Figure 3 describes the details of the model processes and their interconnections at each subcatchment level.

The modified SWAT model has been structured to allow changes/trends in land use, groundwater extraction and hydrologic engineering (village tanks/ponds storages) of the catchment to be easily included in the model as a time series input so that the spatial and temporal variations (dynamic changes) in the input data can be updated during model simulations. Continuous information on land use and watershed development structures can be updated between years based on the available annual information via linear interpolation.

The Soil Conservation Service Curve Number (SCS-CN) method was used to generate surface runoff in each HRU with the remaining water being infiltrated through the multilayer soil profile modelled using the SCS-CN equations (2:1.1.1, 2:1.1.2 and 2:1.1.3 in the SWAT Theoretical Manual) as used in SWAT (Arnold et al., 1998). Generally, the CN values for a given soil, land cover and land management condition are chosen from a table provided in the SWAT model documentation. Hydrologic soil types C and D represented the majority of the HS catchment soils, which were clayey (70%) and loamy (15%). The curve number (CN) of a

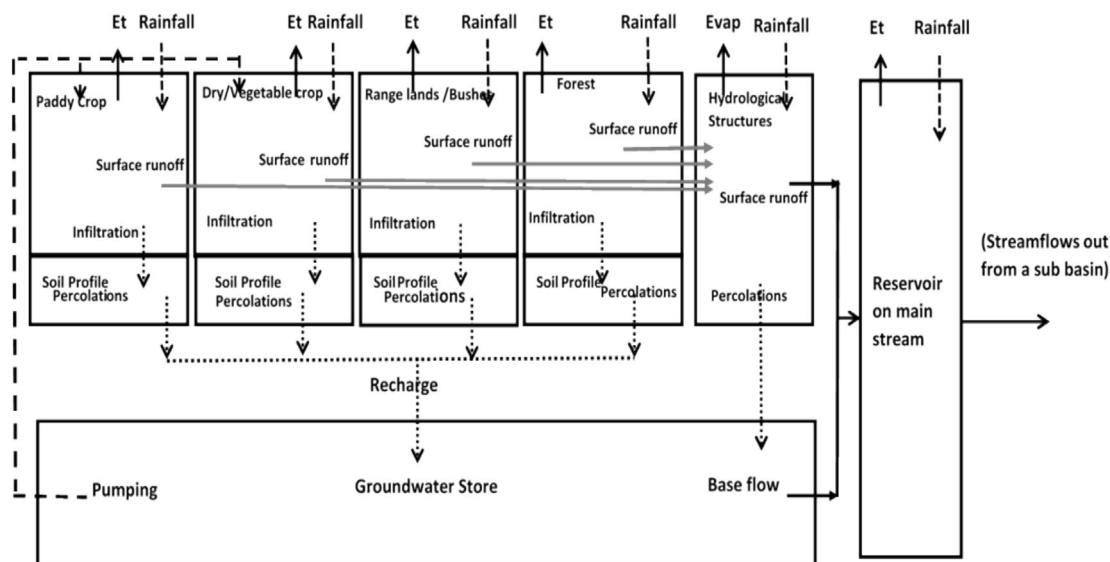


FIGURE 3 Structure of the modified SWAT model.

given day is calculated by using a retention parameter, which changes with the soil water content of the soil profile as per the 5-day soil antecedent moisture conditions (AMCs) (Neitsch et al., 2009). The runoff generated in each HRU is first captured by the watershed development structures within the HRU, and then any spills go into the storage reservoir located at the end of each sub-basin. In addition to overflow from HRUs within a sub-basin, streamflow from the upstream sub-basin will also join the reservoirs in each sub-basin. Furthermore, the reservoir spills are routed downstream through the stream network using a cascade of two linear store approaches and eventually reach the catchment outlet (Figure 3) (Jayatilaka et al., 2003; Ramabrahmam et al., 2021).

Unlike SWAT, the groundwater system is modelled at the subcatchment level rather than at the HRU level, as the contribution of groundwater storage to irrigation depends on the areas in each HRU and their storage capacities, leading to nonlinearity in the groundwater response to recharge and groundwater extraction in a sub-basin. The majority of groundwater resources are present in unconfined shallow aquifers supported by Archaean granite rocks 20–40 m below subsurface profiles (Dewandel et al., 2006). Piezometric gradients indicate that the groundwater flows from west to east, similar to the surface catchment. The direction of groundwater flow and the boundaries of the surface catchment show that the groundwater basin and the surface catchment are closely aligned with one another (Massuel et al., 2013). Since the HS watershed is located upstream of the Musi river basin, the base flow into the catchment was considered to be zero. The groundwater storage in January 1980 was considered the initial level of groundwater storage at

the start of the simulation in the groundwater budget. The groundwater model has a threshold for groundwater storage below which the base flow becomes zero. Since groundwater extractions in irrigated sub-basins may lead to the depletion of groundwater storage below this threshold, the base flow from this sub-basin can reach zero. An area-weighted average of recharge from all the HRUs in a sub-basin is calculated and added to the groundwater storage. This recharge includes vertical soil drainage and seepage from hydrological structures. The base flow contribution to streamflow was calculated using a base flow recession constant (ALPHA\_BF) for all sub-basins. The area-weighted average groundwater storage depth from all sub-basins was calculated and converted into the average groundwater level by assuming a specific yield of 0.02 to enable comparisons against groundwater level observations (Nune et al., 2021).

The irrigation module operates only during the crop-growing period, which is the period from planting to maturity, that is, until the accumulated heat units reach the threshold value (at maturity). The HRU is designed as a depression storage (Programed in the modified SWAT) unit for paddy crops with a defined storage capacity and a threshold level below which autoirrigation is triggered. In the case of non-paddy and vegetable crop HRUs, autoirrigation is triggered when the soil moisture storage in the root zone falls below a threshold level during the crop period, and the HRUs are irrigated to the soil field capacity. The total quantity of water required for irrigation to all HRUs in a sub-basin is deducted from the groundwater storage of that sub-basin.

The total HS catchment area was divided into 19 sub-basins based on the delineated drainage network using

the DEM (digital elevation model). The land use details for each sub-basin for the years 1985, 2000 and 2007 were extracted from the *mandal* (subdivision of district area) land use statistical data obtained from the Department of Economics and Statistics (DES), Telangana state. Based on the spatial distributions of the land use classes and soil types, 41 unique soil–land use combinations (HRUs) were defined, and the areas of each HRU in each sub-basin were extracted. The HRU area fluctuates yearly based on changes in land use in each sub-basin without exceeding the total area of the HS catchment region.

The HS catchment was characterized by four soil layers of varying thickness. In the study area, the south-west monsoon (June–September) subsides completely by the end of October, and the soil water content exceeds the field capacity for that month. Since the model run starts in January, we expected the soil water content to be less than the field capacity. The model calculates the next day's soil water content based on the irrigation provided to the crop, rainfall amount and previous soil moisture content, as crops are usually irrigated in this study area during the *rabi* (post-rainy) season. Based on field experience, observations and field visit discussions with farmers during collection of the data required to build the model, the total available water content at that time of the year is estimated to be 75% of its maximum total available water. The maximum total available water for the plant was calculated as the difference between the field capacity and wilting point water content multiplied by the root zone depth.

In the HS catchment, there are two cropping periods: the *kharif* (rainy) season (paddy crop: July to November; sorghum: July to mid-November; vegetables: July to December) and the *rabi* season (paddy and vegetable crops: January–April). The crop season dates were fixed throughout the simulation runs. The parameters required for crop growth in the modified SWAT model were obtained from the SWAT database. The major crops cultivated in the catchment during *kharif* and *rabi* are rice (rice, as an irrigated crop), sorghum (*grsg*, as a rainfed crop) and tomato (*toma*, as an irrigated vegetable crop). To differentiate irrigated from rainfed areas during the *kharif* and *rabi* seasons, each irrigated area in *kharif* was divided into two parts (two HRUs) so that the *rabi* area could be accommodated within the *kharif* area, one that is irrigated during both the *kharif* and *rabi* seasons and the other that is irrigated only in the *kharif* season.

Based on area–stage–volume relationships collected from a few village water bodies/natural water tanks, all the water bodies in a sub-basin were aggregated (areas and capacities) and represented as a single reservoir in each sub-basin. All the small watershed hydrological structures (check dams, percolation tanks, farmponds,

etc.) located within the sub-basin were aggregated and redistributed as small reservoirs within each HRU in proportion to the HRU areas. The streamflow from the most downstream sub-basin is compared to that in the HS reservoir at the end of the catchment. In this paper, all hydrological water balance component units are expressed in terms of depth relative to the corresponding average annual rainfall over the period. All the catchment characteristics and their spatial and temporal changes were captured as realistically as possible in the model.

### 3.2 | Model calibration

The model was calibrated during 1980–1989 and validated for the period 1990–2007, as the data indicate a low level of water resource development and represent equilibrium conditions at the start of the subsequent development phase, which shows significant land use changes and water resource development (since the 1990s). This period after 1989 has hydrological data that carry a high uncertainty level due to farmers' intervention and interception of surface runoff.

There are a variety of approaches that could be taken to simulate all the changes in the catchment, for example adding one change at a time and gradually building up all changes or simulating all changes in the catchment as realistically as possible and then looking at subsets of change. In this study, the second approach was used by first evaluating the model's ability to simulate change by incorporating all changes and then evaluating the individual changes within the catchment. Finally, the role of different drivers of change on the overall hydrologic change in the catchment was explored.

A range of key model parameters influencing surface runoff generation and groundwater recharge were calibrated in a systematic order. The key parameters used in the model calibration were the soil available water content (Sol\_AWC), soil hydraulic conductivity (Sol\_K), curve number (CN) of the hydrological structures and reservoirs (Structures\_K and Reservoirs\_K), base flow recession constant (ALPHA\_BH) and groundwater delay time (GW\_DELAY). The parameter value ranges were obtained from a calibrated SWAT model that was used in the Osman Sagar catchment, which is another subcatchment of the Musi river that is adjacent to the HS catchment (Garg et al., 2012; Water Technology Centre, 2008). These parameters were systematically adjusted during model calibration. The calibration aimed to match the monthly simulated streamflow with the observed streamflow in the HS reservoir. The details of the initial and final calibrated parameters and their ranges are given in Table 1.



**TABLE 1** Calibrated parameters: initial range and final values.

Parameter	Initial values (range)	Final/calibrated values	Source
Sand content (SAND, %)	23–63	23–63	(Garg et al., 2012; Water Technology Centre, 2008).
Silt content (SILT, %)	5.9–17.8	5.9–17.8	
Clay content (CLAY, %)	22–49.9	22–49.9	
Gravel fraction (ROCK, %)	10–15	10–15	
Bulk density (SOL_BD, g cm <sup>-3</sup> )	1.16–1.53	1.16–1.53	
Soil depth (Z, mm)	400–1,360	400–1,360	
Soil available water content, Sol_AWC (%)	0.13 ± (0.05–0.20)	0.10–0.23	Calibrated
Saturated hydraulic conductivity, Sol_K (mm h <sup>-1</sup> )	2.0 ± (1.0–8.0)	6–6.5	Calibrated
Curve number, CN	(70–80) ± (2–20)	54–74	Calibrated
Soil evaporation compensation coefficient, ESCO	0.8 ± (0.05–2.0)	0.9	Calibrated
Hydraulic conductivity of the structures bottom, Structures_K (mm h <sup>-1</sup> )	4 ± (0.25–5)	6.25	Calibrated
Hydraulic conductivity of the reservoir bottom, Reservoirs_K (mm h <sup>-1</sup> )	2 ± (1.0–5.0)	3	Calibrated
Base flow recession constant, ALPHA_BF	0.005–0.02	0.02	Calibrated
Groundwater delay time (days), GW_DELAY	22	22	Calibrated

### 3.3 | Model validation

The following scenarios were created to evaluate the model's capacity to capture all watershed changes and to attribute the trends in streamflow and groundwater storage to their historical changes:

- Base case (Base): A scenario with changes in meteorological data but without any changes in catchment characteristics observed during calibration.
- Stationary climate (SC): A scenario that is the same as the Base case scenario but forced with a detrended (with only the trend in observed meteorological parameters removed) time series of wind speed and relative humidity data over the entire simulation period.
- Water harvesting (WH): A scenario that is the same as the Base case scenario except that it considers changes in watershed development structures (small and village tanks) that occurred over the entire simulation period.
- Land use change (LU): A scenario that is the same as the Base scenario but only considers land use changes that occurred during the entire simulation period; and
- Best estimate (Best): A scenario that closely captures catchment reality with observed changes in both climate and catchment characteristics.

In the ideal estimate (Ideal) scenario, to integrate the impacts of both climate and catchment changes, the observed meteorological data, changes in land use

and watershed development structures during the validation period were input into the model.

### 3.4 | Future climate change scenarios

A set of Quantifying Uncertainties in Model Predictions (QUMP) ensembles under the A1B emission scenario was selected for this study. The ensembles were generated by the Hadley Centre Coupled Model, version 3 (HadCM3-version 3) using the Special Report on Emission Scenarios (SRES) A1B emission scenarios provided by the Intergovernmental Panel on Climate Change (IPCC, 2007) over the South Asian domain. HadCM3 is a coupled atmospheric–ocean general circulation model, and a detailed description of the model was provided by Gordon et al. (2000) and Pope et al. (2000). The QUMP ensemble data sets of HadCM3 were validated for the Indian subcontinent and downscaled using PRECIS by the Indian Institute of Tropical Meteorology (IITM), Pune, India. This generated high-resolution (50 × 50 km) data for the period 1961–2098 for the Krishna river basin (Kumar et al., 2011). PRECIS (Providing Regional Climates for Impact Studies) is a regional climate model developed by the UK Meteorological (Met) Office at the Hadley Centre and has been applied in many regions of the world. A detailed description of the PRECIS model was provided by Jones et al. (2004). The daily gridded rainfall data produced by the India Meteorological Department (hereafter IMD) for the period 1961–1990 were used

to validate the performance of the PRECIS data in reproducing historical climate data (Rajeevan et al., 2006). In all the simulations, the spatial distributions of rainfall and surface air temperature over the Krishna basin were satisfactorily simulated in the Q0, Q1 and Q14 data sets. However, two QUMP simulations, Q0 and Q14, showed a wetter bias, and Q1 produced a dry bias over the entire basin. The simulated climate (Q0, Q1 and Q14) data of each grid spread over the HS catchment were averaged for each component and given as input to the model.

Quantile mapping can be classified as distribution-based (calibrated on climatological distributions rather than on paired data), direct (predictor and predictand are the same parameters), or parameter-free (using empirical cumulative density distributions, *ecdfs*, rather than theoretical cumulative distribution functions). In this study, QM was applied to daily ( $t$ ) data for each grid cell ( $i$ ), resulting in a corrected time series ( $Y_{cor}$  in Equation 1), which was obtained using a correction function (CF) defined in Equation (2):

$$Y_{t,i}^{cor} = X_{t,i}^{raw} + CF_{t,i} \quad (1)$$

$$CF_{t,i} = ecdf_{doy,i}^{obs,cal-1}(P_{t,i}) - ecdf_{doy,i}^{mod,cal-1}(P_{t,i}) \quad (2)$$

$$P_{t,i} = ecdf_{doy,i}^{mod,cal}(X_{T,i}^{raw}) \quad (3)$$

The CF represents the difference in the probability  $P$  between the observed and modelled (*mod*) inverse *ecdf* data (*ecdf*−1) for the respective day of the year (*doy*) within the calibration period (*cal*) (Kundzewicz & Robson, 2004).  $P$  is obtained by relating the raw climate model output  $X_{raw}$  to the corresponding *ecdf* in the calibration period. For QM calibration, data from 1969 to 2004 are used for a 31-day window centred on *doy*.

### 3.5 | Future anthropogenic changes

The trends observed in anthropogenic changes during 1980–2007 were used as the basis for developing future changes in land use, water storage structures (e.g. reservoirs) and water-harvesting structures (small watershed structures), as shown in Table 2. In 2014–2015, the Mission Kakatiya programme was launched to desilt soil from existing village water tanks to increase their water storage capacity and to recharge groundwater storage around them. It was estimated that the area of village water tanks increased by 20% (2018) compared with that in the pre-Mission Kakatiya programme (Gumma et al., 2023). The storage capacities of these village water storage tanks are expected to increase by 50% (by 2020), as both the capacity and storage area of the existing storage tanks have been observed to increase through the Mission Kakatiya programme. Therefore, in this model, the storage capacity of these tanks will increase by 50% by 2020 and remain the same until the end of the century (2098).

This study predicts that the Telangana government will continue to implement soil and rainwater conservation programmes (watershed structures) that will lead to future land use changes. The storage capacity of small watershed structures is projected to double by 2040, quadruple by 2070 and increase by a factor of 5.7 by 2098. Therefore, the area under irrigated crops is expected to increase with the same trend observed historically. However, the expansion of irrigated crops is expected to occur initially in rainfed areas and later spread to uncultivable areas. Since groundwater is already depleted in the HS catchment, the irrigated area is likely to increase at a rate of 100 km<sup>2</sup> every 30 years, as the groundwater levels in the HS catchment have been depleting since 2000, and the growth rate of irrigated crop area is

**TABLE 2** Details of changes during the period from 1980 to 2098; res. capacity = reservoir capacity; HS capacity = hydrologic structure capacity.

Changes	Area (km <sup>2</sup> )	1980	1990	2000	2010	2040	2070	2098
Land use (km <sup>2</sup> )	Forest	65	65	67	67	67	67	67
	Uncultivable	695	695	695	695	672	649	626
	Rainfed	494	494	407	312	235	158	96
	Irrigated	45	45	130	225	325	425	510
	Total area	1,299	1,299	1,299	1,299	1,299	1,299	1,299
Res. capacity	Surface area	13	13	13	13	20	20	20
	Volume (ML)*	18,280	18,280	18,280	18,280	27,420	27,420	27,420
HS capacity	Surface area	0.00	0.60	1.8	2.8	4.8	6.8	8.5
	Volume (ML)	0.00	1,176	3,399	5,300	8,967	12,634	16,300

\*Million litres.

observed to be 90 km<sup>2</sup> every 10 years (1990–2000: 85 km<sup>2</sup>; 2000–2010: 95 km<sup>2</sup>, an average of 90 km<sup>2</sup> every 10 years).

### 3.6 | Future simulations

The modified SWAT model, which was calibrated and validated against historical streamflow and groundwater storage in the HS watershed, was used to evaluate the impact of future anthropogenic changes by applying three future climatic simulations (Q0, Q1 and Q14). The following scenarios were generated to assess the individual impacts of future climate and anthropogenic changes on the hydrology of the HS catchment. In scenario 1, to analyse the impact of climate change in the future, the model is forced with future climate data without changing the characteristics of the HS catchment during the entire simulation period (2011–2098). In scenario 2, to analyse the impact of both climate and catchment changes (such as land use, watershed water-harvesting strictures, village water tanks and naturally formed lakes) in the future, the model is forced with future climate and anthropogenic changes in the catchment. Finally, two scenarios were used to analyse the combined and individual impacts of both climate and anthropogenic changes on the HS hydrological system.

## 4 | RESULTS

During the calibration period (1980–1989), good agreement was observed between the simulated and observed monthly and annual streamflows ( $R^2$  (coefficient of determination) = 0.85 and 0.97, Nash–Sutcliffe model efficiency = 0.83 and 0.92, (Nash & Sutcliffe, 1970), respectively) (Figures 4a–c). During the calibration period, the average annual simulated streamflow was 82 mm, 44 mm of which was from surface runoff and 38 mm from base flow. Similarly, during this period, the average annual irrigation depth extracted from groundwater resources for the entire HS catchment was estimated to be 61 mm. The average annual recharge to groundwater storage due to rainfall and irrigation of 715 and 61 mm, respectively, was simulated to be 99 mm. The average annual actual evapotranspiration (ET) for the entire HS catchment was 634 mm. There was no trend in the simulated annual groundwater level of the HS during the calibration period 1980–1989 (Figure 4d).

During the validation period, the average annual simulated and observed streamflow (1980–2007,  $R^2 = 0.90$ , NSE = 0.86) at the HS reservoir showed a good correlation (Figures 5a, b), and this scenario provided the best predictions of streamflow along with the land use change scenario. Ragab et al. (2020), using five catchment river flows in the UK, found that the lowest uncertainty in

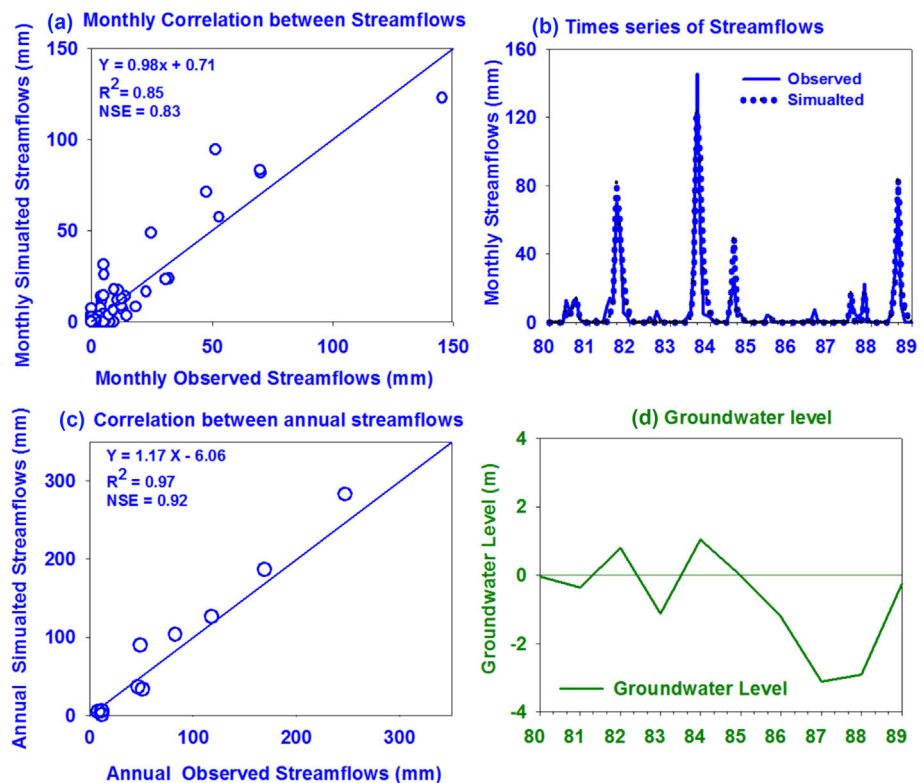


**FIGURE 4** Model results for the calibration period: (a) scatter plot of monthly simulated and observed streamflow data, (b) time series of monthly observed and simulated streamflow data, (c) scatter plot of annual simulated and observed streamflow data, and (d) average annual groundwater level at the start of each year (January) during the calibration period (1980–1989).

predicted river flows when increasing the timescale from daily to monthly to seasonal was associated with annual flows. Daily and monthly data commonly have more noise (sudden peaks and drops), while annual flows integrate, harmonize and smooth out such sudden variations.

During the validation period, the streamflow into the HS reservoir from the catchment decreased drastically compared with that during the calibration period (80 mm). The average annual streamflow observed in the HS reservoir was 39 mm, whereas the model-simulated streamflow was 36 mm. Due to changes in land use and increased watershed development structures, groundwater extraction for irrigation increased, on average, to 104 mm. Similarly, the average annual recharge and average annual actual evapotranspiration of the catchment increased to 105 and 699 mm, respectively (Figures 5c–f).

Due to all changes in the HS catchment during the study period (1980–2007), the rate at which the observed streamflow declined was  $-3.03 \text{ mm yr}^{-1}$ , whereas the simulated streamflow declined at a rate of  $-2.65 \text{ mm yr}^{-1}$ . Similarly, it was observed that the average groundwater levels declined at a rate of  $0.19 \text{ mm yr}^{-1}$  during the

validation period (1990–2007). The rate of groundwater depletion observed in this study (subcatchment of the Musi river basin) is similar to that of the larger Musi catchment, where the groundwater level declined at a rate of  $0.18 \text{ m/year}$  (1998–2004) (Massuel et al., 2013). Overall, the best estimate scenario led to the greatest decline in streamflow and the second greatest decline in groundwater levels in the catchment.

#### 4.1 | Changes in PRECIS climate data before and after bias corrections

Daily meteorological data of each grid covering the study area obtained from the Indian Meteorological Department (IMD Pune, India) were used for bias correction of three PRECIS future climate projections (Q0, Q1 and Q14). The period 1980–2010 was selected as the baseline period in this study because the study used the period 1980–89 for calibration and the period 1990–2007 for validation of the modified SWAT model. Model results were analysed to assess the impacts of future climate and anthropogenic activities on streamflow and groundwater

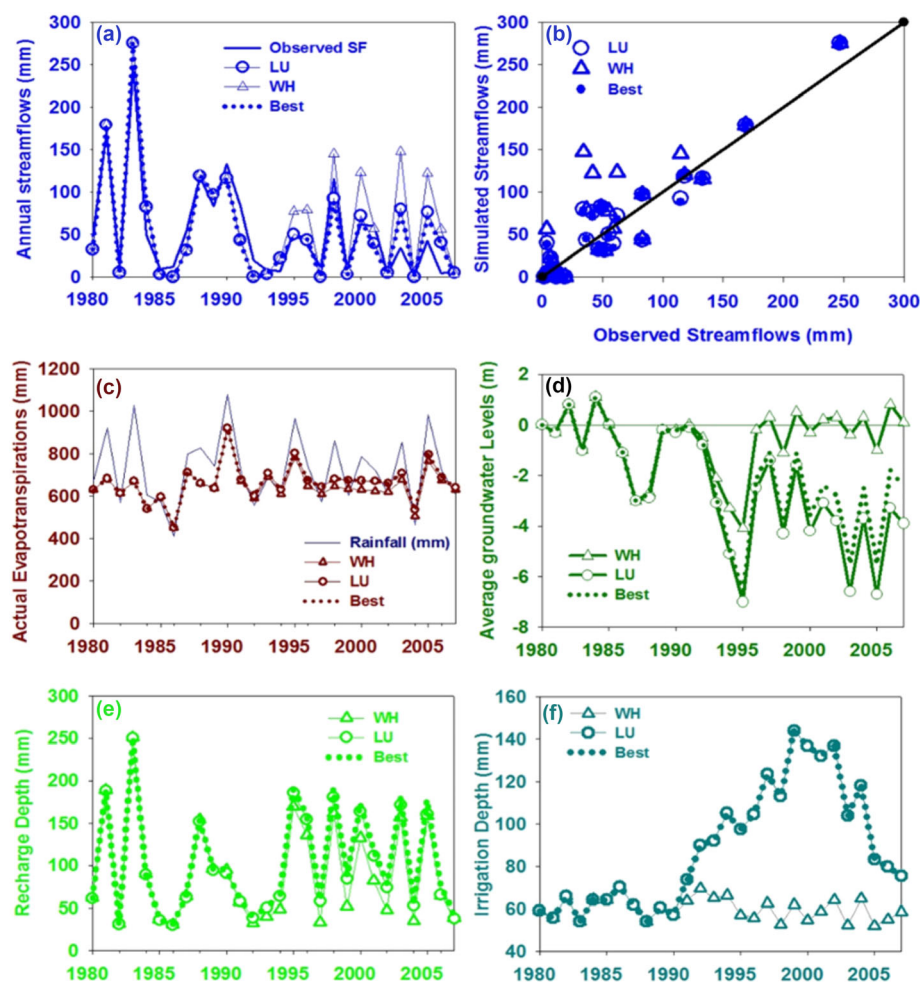


**FIGURE 5** Trends of hydrological processes in different scenarios (WH, LU & Best): (a) observed and simulated streamflow; (b) correlation between observed and simulated streamflow; (c) actual evapotranspiration; (d) groundwater levels; (e) groundwater recharge and (f) irrigation depths in the Himayat Sagar catchment.

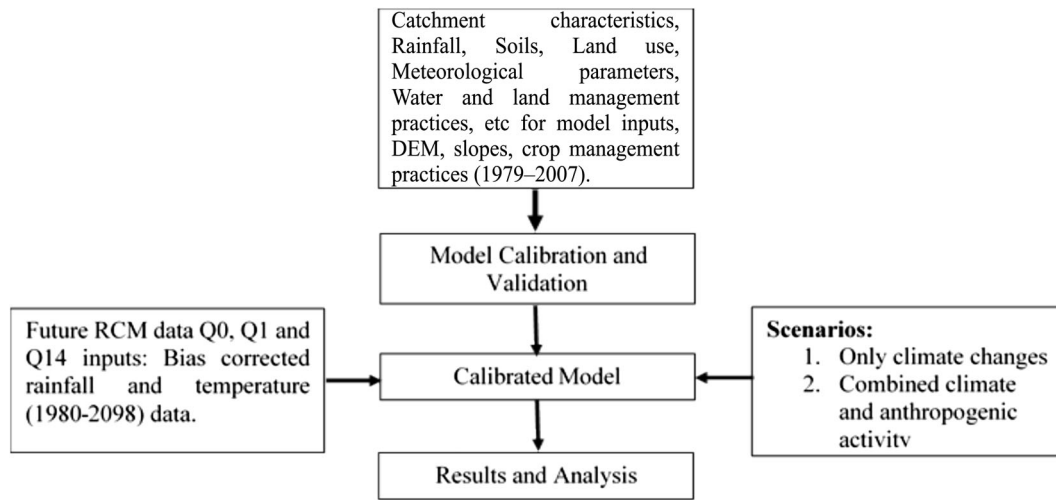
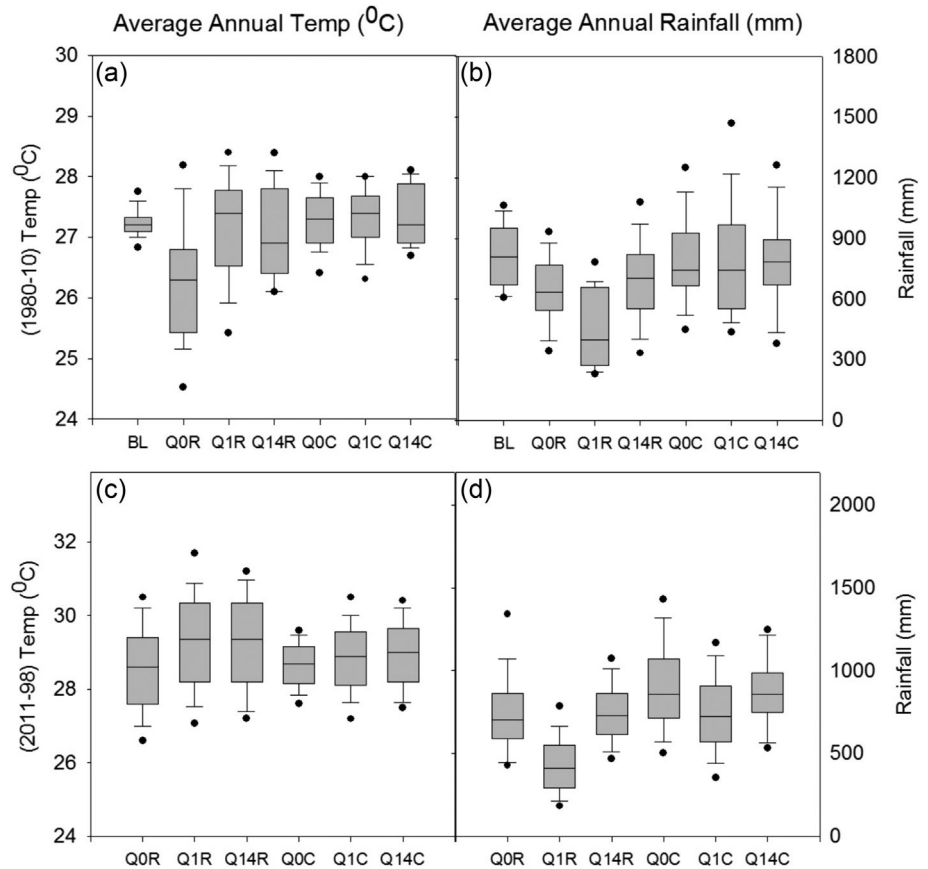


**FIGURE 6** A framework of model set-up and processes for analysing the impact of climate change and anthropogenic activity on catchment hydrology.

**FIGURE 7** Comparison of the Q0, Q1 and Q14 climate projections before (R) and after bias correction (C) using the observed IMD data: (a) and (b) average annual temperature and rainfall data for the period 1980–2010, and (c) and (d) average annual temperature and rainfall data for the period 2011–2098. The lower whisker indicates minimum rainfall (excluding outliers), and the upper whisker indicates maximum rainfall (excluding outliers).



storage for each climate condition for each time slice (early: 2011–2040, middle: 2041–2070 and end century: 2071–2098) as shown in Figure 6.

Figure 7 shows the changes in the average annual temperature and rainfall before and after bias correction of the future-projected data to the IMD observed data. The difference between the average annual temperatures

during the baseline period (1980–2010) was negligible: 27.1°C for the IMD data and 27.4°C (Q0), 27.4°C (Q1) and 27.2°C (Q14) for the predicted climate data (Figure 7a). Similarly, the projected average annual rainfall was slightly (3–12%) greater than the observed historical rainfall, indicating no significant differences in the data (Figure 7b). The average annual rainfall during the

**TABLE 3** The average annual temperatures (°C) according to the IMD (India Meteorological Department) (observed) and PRECIS (Providing Regional Climates for Impact Studies) raw and bias-corrected (Cor.) data for different time slices. (Note: Obs. is observed; Diff. means difference.)

$T_{avg}$	Obs.	Q0 Raw	Q0 Cor.	Q0 Diff.	Q1 Raw	Q1 Cor.	Q1 Diff.	Q14 Raw	Q14 Cor.	Q14 Diff.
1961–1990	27.10									
1980–2010		26.28	27.35		27.42	27.35		26.87	27.18	
2011–2040		27.44	28.06	0.7	27.95	27.90	0.6	28.04	28.05	0.9
2041–2070		28.59	28.63	1.3	29.47	29.04	1.7	29.59	29.09	1.9
2071–2098		29.63	29.27	1.9	30.50	29.76	2.4	30.50	29.79	2.6

**TABLE 4** The average annual rainfall (mm) of the IMD (India Meteorological Department) (observed) and PRECIS (Providing Regional Climates for Impact Studies) raw and bias-corrected (Cor.) data for different time slices. (Note: Obs. is observed; Diff. means difference.)

Median values	Obs.	Q0 Raw	Q0 Cor.	Q0 Diff.	Q1 Raw	Q1 Cor.	Q1 Diff.	Q14 Raw	Q14 Cor.	Q14 Diff.
1961–1990	803									
1980–2010		634	790		398	791		702	786	
2011–2040		614	792	2(0.3%)	470	817	26(3.3%)	754	879	93 (11.8%)
2041–2070		721	989	199 (25.2%)	361	693	−98(−12.4%)	722	844	58(7.4%)
2071–2098		749	948	158 (20.0%)	401	727	−64(−8.1%)	704	896	110 (14.0%)

baseline period from the projected data was 790 mm (Q0), 791 mm (Q1) and 786 mm (Q14), while it was 803 mm from the observed average annual rainfall (IMD) data (Tables 3 and 4 and Figure 7). Overall, during the baseline period, the bias-corrected average annual temperature and rainfall (bias-corrected Q0, Q1 and Q14) showed good agreement with the observed data (Figures 7c, d). There are very few differences in the mean annual temperature and rainfall between the observed and corrected data. Therefore, bias-corrected data from 1980 to 2098 were used as inputs to the modified SWAT model to maintain consistency and compatibility and to compare the impacts of climate changes from the baseline to the early–middle–end centuries for each climate projection (Q0, Q1 and Q14).

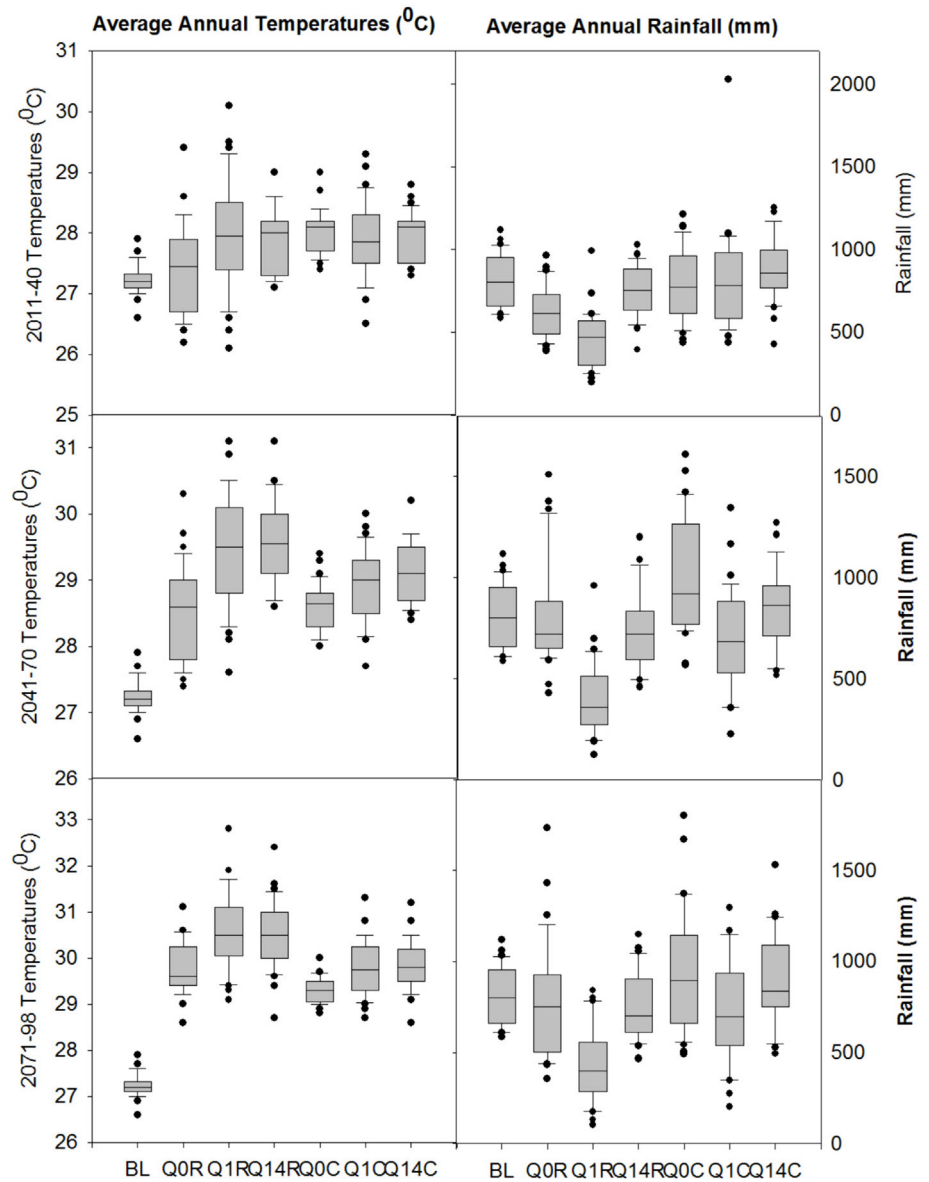
Model simulations for three time slices of three future climate projections are compared to their baseline periods. In all cases, a continuous significant increasing trend of 0.6–0.9°C in mean annual temperatures was observed by the end of the century relative to their baseline (for the early, middle and end time slices: 0.7, 1.3 and 1.9°C for Q0; 0.6, 1.7 and 2.4°C for Q1; and 0.9, 1.9 and 2.6°C for Q14), as shown in Table 3. However, the average annual rainfall in the early, middle and end centuries differed from the baseline in each climate projection. In the Q0 climate projection, a continuous increasing trend in the average annual rainfall is observed from the beginning to the end of the century

(0.3% (early), 25.2% (middle) and 20.1% (end)). In contrast, in the Q1 climate projection, the average annual rainfall increased by 3.3% in the early century and decreased by 12.4% (middle) and 8.1% (end) by the end of the century. In the Q14 climate projection, the average annual rainfall increased by 11.8% (early), 7.4% (middle) and 14.0% (end) compared to that in the baseline period (Table 4 and Figure 8).

## 4.2 | Seasonal variation in climate data

Seasonal and monthly climate data were analysed to understand their variations in each climate projection. Towards the end of the century, the maximum monthly rainfall was observed to shift from August to September (Figure 9). From the baseline period to the early century, August was recorded as the month with maximum rainfall in all climate projections (except for 60 mm higher rainfall in Q14 than in the other climate projections). In the middle century, increases in rainfall in August of 43% (247 mm) and 30% (224 mm) were observed in both the Q0 and Q14 projections, respectively. However, during the end of the century, an increase in rainfall was observed in all monsoon months (June, July, August and September, JJAS) in the Q0 projections, and it was also observed that the maximum rainfall in the season clearly shifted from August to September (Figure 9). The

**FIGURE 8** Mean and extreme values of average annual temperature before and after bias correction for all three time slices and climate projections. The lower whisker indicates minimum temperatures (excluding outliers), and the upper whisker indicates maximum temperatures (excluding outliers).



projected future mean surface temperatures are observed to increase significantly compared to the baseline at all time points in all three climate projections. However, no major shifts in the seasonal temperature from the average monthly temperature were observed (Figure 9).

### 4.3 | Hydrological impacts due to climate and anthropogenic changes

The scenarios discussed in the model validation section are the scenarios used to validate the simulations of the modified SWAT model against observed historical streamflow and groundwater resources. On the other hand, the scenarios included in this section are meant to evaluate how future modifications would affect the hydrology of the HS catchment.

#### 4.3.1 | Baseline period (1980–2010)

To analyse the impacts of future climate and anthropogenic changes, the baseline period of each climate projection from 1980 to 2010 was selected as the base for comparing hydrological changes in their future time slices instead of the observed historical data. That is, the average annual values of all hydrological processes for each time slice (early, middle and end century) in each climate projection (Q0, Q1 and Q14 simulations) were compared with their corresponding baseline period values. For detailed analysis, the average annual rainfall of each time slice is partitioned into the following water balance components: average annual streamflow (SF = surface runoff + base-flow), average annual actual evapotranspiration (AEt), average annual change in groundwater storage (CGWS) and average annual change

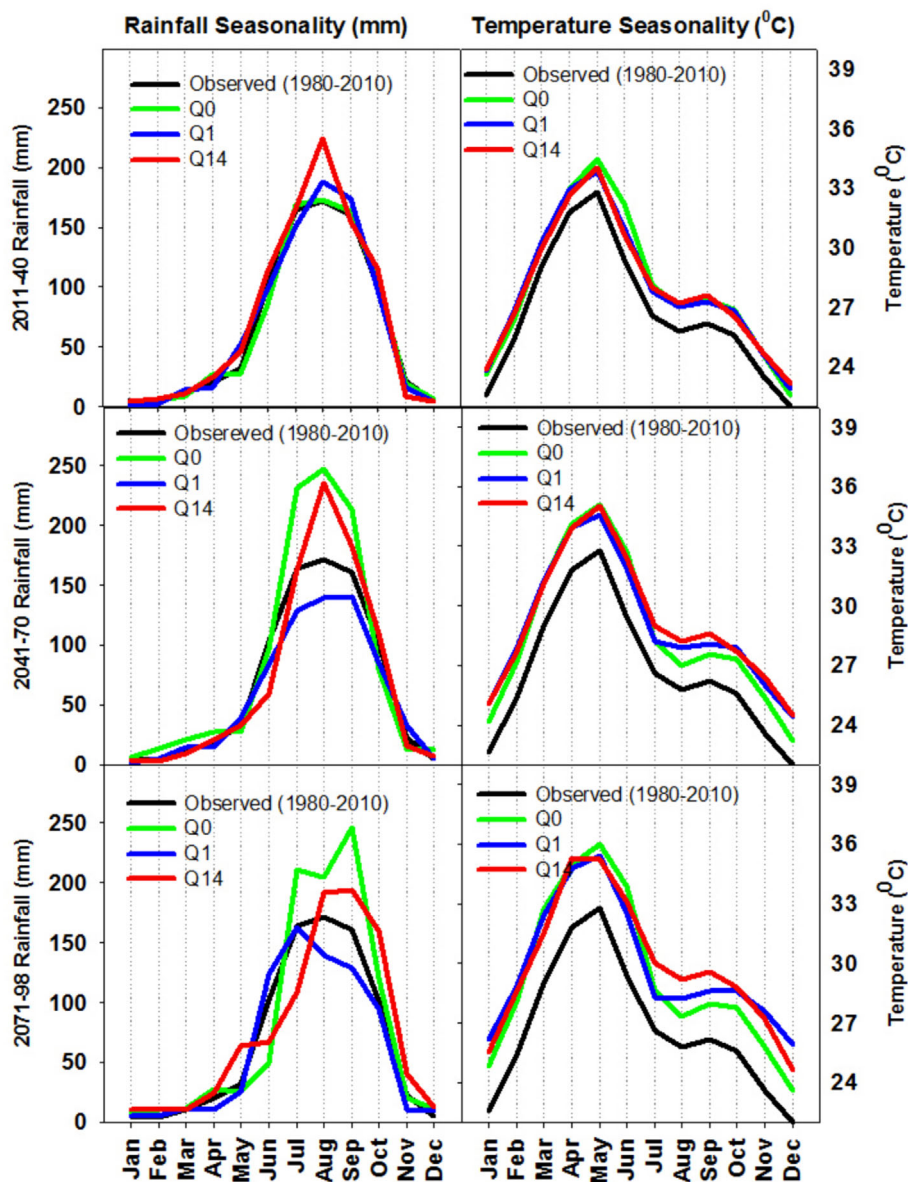


FIGURE 9 Seasonality of mean monthly rainfall and temperatures for three time slices for three climate projections compared with IMD-observed data (1961–2006).

in other stores (CHANGES, changes in sum of stores in reservoirs, hydrological water-harvesting structures, depressions and soil). Table 5 indicates the percentage change in water balance components during each time slice for each climate projection.

During the baseline period, major changes in hydrological responses were detected only in SF and AEt in all three climate projections (Q0, Q1 and Q14). The average annual rainfall RF (15–21%) is partitioned into SF (19.1, 14.7 and 21.3%; surface runoff: 7.0, 6.8 and 7.4%; and base flows: 12.1, 7.9 and 13.9%) and 79–84% AEt (79.7, 84.4 and 77.6%) for Q0, Q1 and Q14, respectively. However, no changes in groundwater storage (CGWS) or water storage structures (CHANGES) were observed during the baseline period. The proportions of water balance components at different time slices of each climate projection for both the climate change scenario and the combined climate and

catchment change scenario are given in Table 5. The following sections compare the hydrological impacts of climate and catchment changes in the HS catchment for each climate projection for different time slices.

#### 4.3.2 | Early-century (2011–2040)

##### *Scenario 1 Impact of climate change*

During the early century, although the average annual rainfall was different, the average annual temperature increased by 0.7°C under all three climate projections. Compared to the baseline period, the average annual rainfall showed no significant changes in Q0 (0.3%), but a marginal increase was observed in Q1 (3.3%) and Q14 (11.8%) during the early century. In the Q0 climate projection, streamflow (SF) decreased by 13.1%, and actual



**TABLE 5** The average annual rainfall and its key proportions (percentages) for each time slice off the climate projection under only climate change (surf. Runoff = surface).

% of RF	WBC	Baseline	Only climate change			Climate and anthropogenic changes		
		1980–2010	2011–2040	2041–2070	2071–2098	2011–2040	2041–2070	2071–2098
<b>Q0</b>	RF (mm)	790	792	989	948	792	989	948
	SF (%)	19.1	16.6	30.6	29.6	7.8	8.7	9.2
	Surf. Runoff (%)	7.0	5.8	10.7	12.0	4.2	8.0	9.2
	Base Flow (%)	12.1	10.8	19.9	17.6	3.6	0.7	0.0
	AEt (%)	79.7	82.4	68.1	68.6	99.1	92.4	102.4
	CGWS (%)	−1.1	−1.0	−0.9	−0.5	−9.1	−3.1	−13.4
	CHANGES (%)	2.3	2.0	2.2	2.3	2.2	2.0	1.8
<b>Q1</b>	RF (mm)	791	817	693	727	817	693	727
	SF (%)	14.7	15.9	8.7	10.6	8.4	4.4	5.1
	Surf. Runoff (%)	6.8	6.6	6.1	7.6	5.0	4.4	5.1
	Base Flow (%)	7.9	9.3	2.6	3.0	3.4	0.0	0.0
	AEt (%)	84.4	83.4	91.0	87.1	102.6	136.6	141.1
	CGWS (%)	−0.8	−1.2	−1.1	1.0	−12.8	−42.7	−47.9
	CHANGES (%)	1.7	1.9	1.4	1.3	1.8	1.7	1.7
<b>Q14</b>	RF (mm)	786	879	844	896	879	844	896
	SF (%)	21.3	24.8	27.0	20.7	11.9	6.9	5.3
	Surf. Runoff (%)	7.4	7.9	9.3	7.9	6.3	6.3	5.3
	Base Flow (%)	13.9	16.9	17.7	12.8	5.6	0.6	0.0
	AEt (%)	77.6	73.9	71.6	77.8	87.7	102.0	110.3
	CGWS (%)	−0.9	−1.0	−0.8	−0.6	−2.0	−10.6	−17.2
	CHANGES (mm)	2.0	2.3	2.2	2.1	2.4	1.7	1.6

Note: RF = rainfall, SF = stream flow, Surf. Runoff = surface runoff, AEt = actual evapotranspiration, CGWS = changes in groundwater storage, CHANGES = water storage structures, and WBC = water balance components.

evapotranspiration (AEt) increased by 3.4%, despite no significant change in average annual rainfall, indicating temporal and quantitative changes in rainfall. In the Q1 and Q14 climate projections, due to the increase in rainfall, streamflow (SF) increased by 8.2 and 16.4%, respectively, and actual evapotranspiration (AEt) decreased slightly by 4.8% (Q14). Overall, in the early century, due to climate change alone, streamflow may change from −13.1 to +16.4%, and actual evapotranspiration may change from −4.7 to +3.4%, but no significant changes in groundwater storage or water storage structures are observed under all climatic conditions (Figures 10–12).

#### Scenario 2 Impact of combined climate and catchment changes

Due to climate and catchment changes, in the early century, streamflow decreased significantly from 47.2 to 53.0%, and actual evapotranspiration increased from 18.7 to 23.0%. However, despite no significant change in catchment stores, a slight decrease in groundwater

storage is observed in all the Q0 (from −1.0 to −9.1%, 71 mm storage or 3.6 m level), Q1 (from −1.2 to −12.8%, 106 mm or 5.3 m) and Q14 (from −1.0 to −2.0%, 18 mm or 0.9 m) projections (Table 5, Figures 10–12).

#### 4.3.3 | Middle century (2041–2070)

##### Scenario 1 Impact of climate change

Compared to the baseline period, during the middle century, the average annual temperature increased more than that in the early century in all climate projections (Q0: +1.3°C, Q1: +1.7°C and Q14: +1.9°C), and the average annual rainfall RF changed from −12.4 to 25.2% (Q1: −12.4%; Q0: +25.2% and Q14: +7.4%). The change in rainfall exhibited a similar change in streamflow (SF) into the HS reservoir (Q1: −40.8%; Q0: 60.2% and Q14: 26.8%), and these changes were offset by changes in actual evapotranspiration (AEt) in all climate projections (Q0: −14.6%, Q1: +7.8% and Q14: −7.7%). Overall,

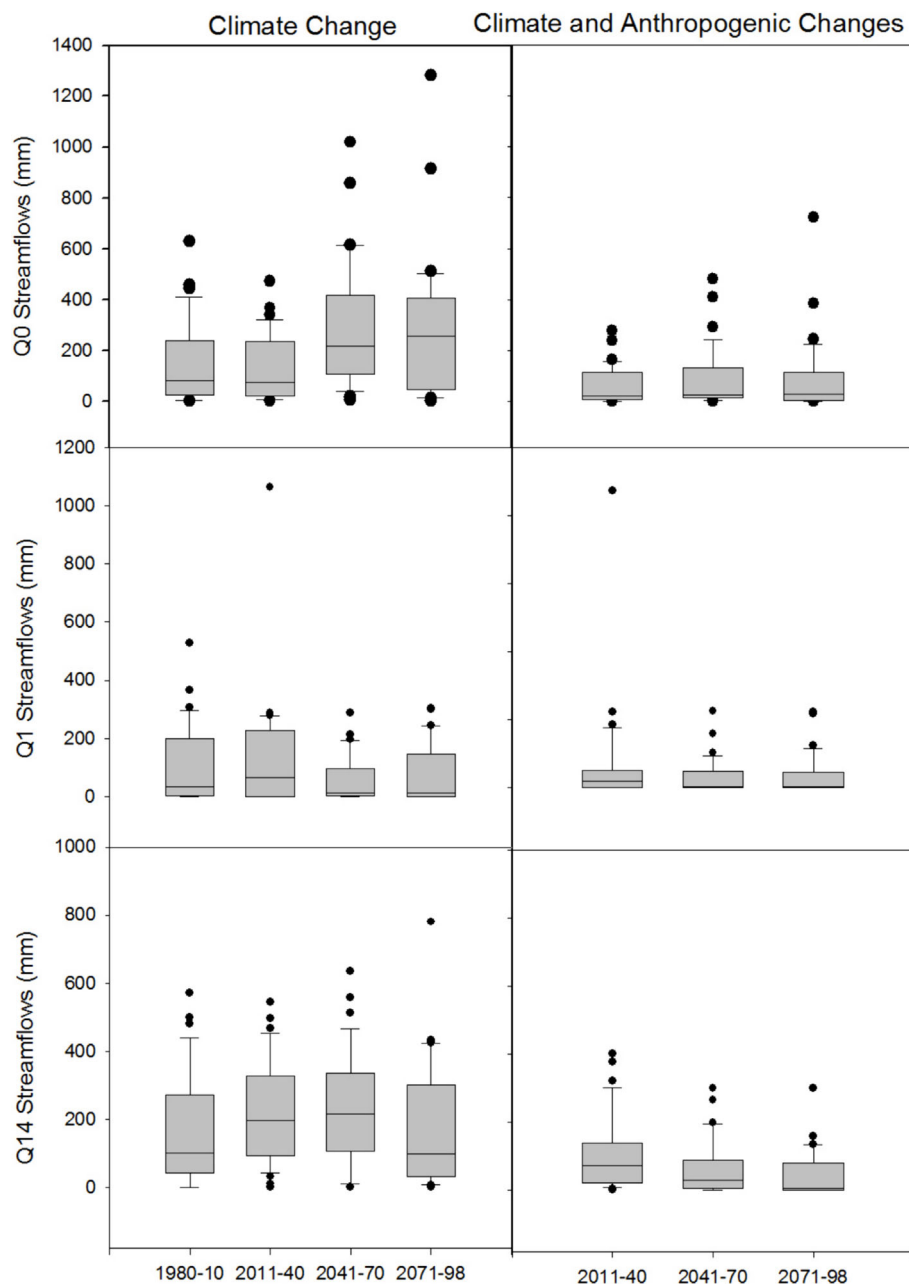


**FIGURE 10** Streamflow in all time slices and climate projections. The left column shows the Himayat Sagar streamflow due to only climate change, and the right column shows the streamflow due to climate and anthropogenic changes.

during the middle century, the HS streamflow could change by  $-40.8$  to  $60.2\%$ , and the catchment evapotranspiration could change by  $-14.6$  to  $+7.8\%$  due to climate change (Figures 10, 12). However, due to climate change, significant changes in groundwater storage (CGWS) and water storage structures (CHANGES) in the HS catchment were not observed (Figure 11).

#### *Scenario 2 Impact of combined climate and anthropogenic changes*

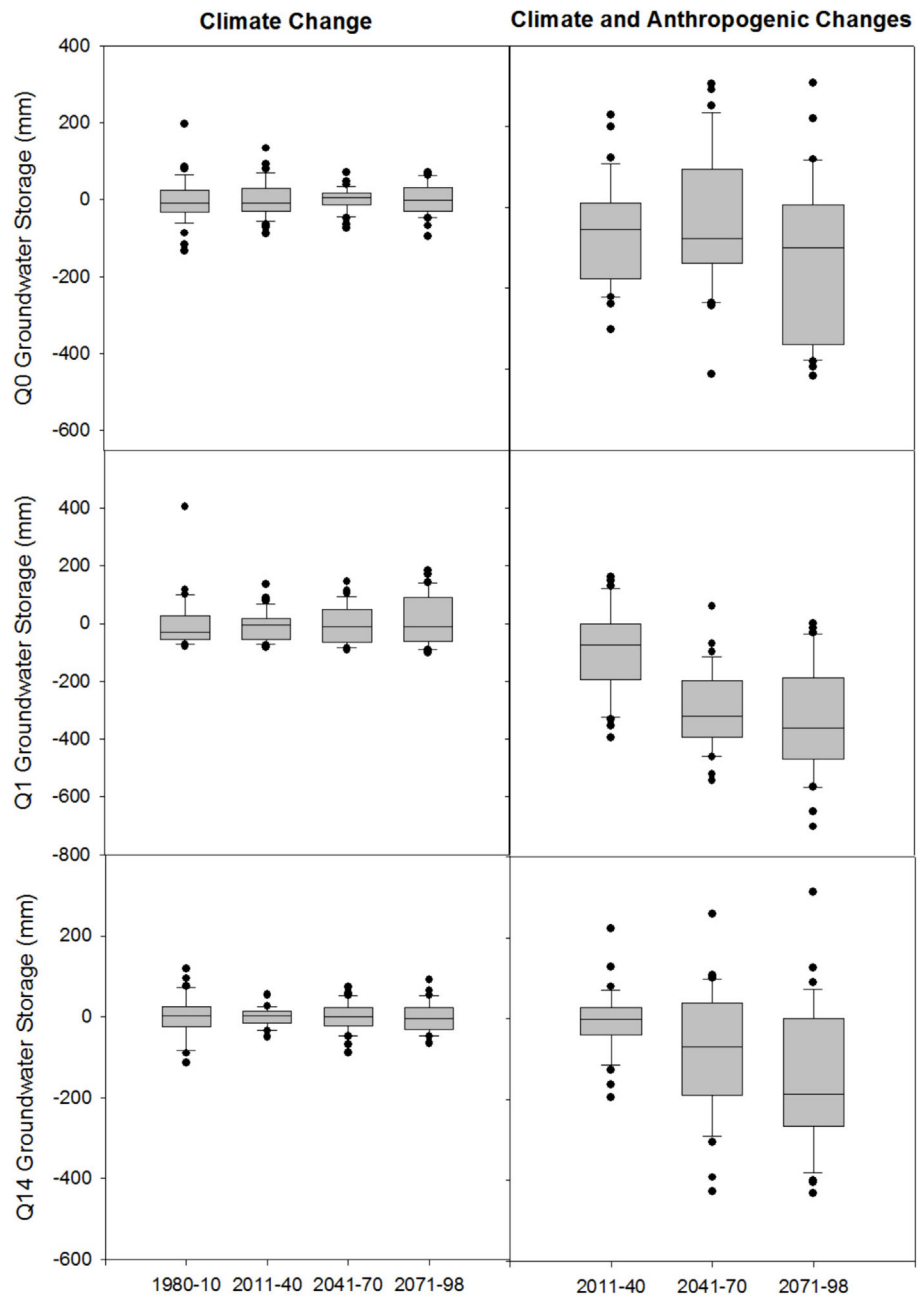
During the middle century, due to climate and anthropogenic changes in the HS catchment, compared to the climate change scenario, streamflow (SF) into the HS reservoir decreased significantly from  $-49$  to  $-74\%$  (Q0:

$-71.6\%$ , Q1:  $-49.4\%$  and Q14:  $-74.4\%$ ), AEt increased by  $35.7$ ,  $50.1$  and  $42.5\%$ , and changes in groundwater storage (CGWS) decreased from  $3.1$  to  $42.7\%$  (Q0: from  $-1.0$  to  $-3.1\%$ ,  $30$  mm storage or  $1.5$  m level, Q1: from  $-1.2$  to  $-42.7\%$ ,  $298$  mm or  $15$  m and Q14: from  $-1.0$  to  $-10.6\%$ ,  $93$  mm or  $4.6$  m) in all the climate projections, as shown in Table 5.

#### 4.3.4 | End century (2071–2098)

By the end of the century, compared to their baseline periods, the average annual temperature is expected to increase by  $2.3^{\circ}\text{C}$ , and the average annual rainfall varies

**FIGURE 11** Groundwater storage in time slices and climate projections. The left column shows changes in the Himayat Sagar groundwater storage due to climate change alone, and the right column shows changes in groundwater storage due to climate and anthropogenic changes.



from  $-8.1$  to  $20.0\%$  (Q0:  $+20.0\%$ , Q14:  $+14.0\%$  and Q1:  $-8.1\%$ ) in the three (Q0, Q1 and Q14) projections.

#### *Scenario 1 Impact of climate change*

Due to climate change alone, the average annual streamflow (SF) during the end of the century varied from  $-27.9$  to  $55.0\%$  (Q14:  $-2.8\%$ , no change, Q1:  $-27.9\%$  and Q0:  $55.0\%$ ). The observed change in HS streamflow (SF) was offset by changes in other hydrological components, such as AEt (Q0:  $-13.9\%$ ; Q1:  $3.2\%$ ; Q14:  $0.3\%$ , no change), CWGS (Q0: from  $-1.1$  to  $-0.5\%$ , no change; Q1: from  $-0.8$  to  $+1.0\%$ , increased by  $15$  mm; Q14: from  $-0.9$  to  $-0.6\%$ , no change) and CHANGES, in the stores (Q0: no changes; Q1: decreased by  $7$  mm; Q14: no change).

#### *Scenario 2 Impact of combined climate and anthropogenic changes*

Due to both climate and anthropogenic changes, streamflow (SF) decreases significantly in all climate projections during the end of the century (Q0:  $-68.9\%$ ,  $194$  mm; Q1:  $-51.9\%$ ,  $38$  mm; and Q14:  $-74.4\%$ ,  $138$  mm), as observed in the middle century. Consequently, due to climate and anthropogenic changes in the HS catchment, during the end of the century, AEt increased from  $41.8$  to  $62.0\%$  (Q0:  $49.3\%$ , Q1:  $62.0\%$  and Q14:  $41.8\%$ ), while changes in groundwater storage (CGWS) decreased between  $6$  m and  $17$  m (Q0:  $-123$  mm or  $6$  m; Q1:  $-349$  mm or  $17$  m and Q14:  $-152$  mm or  $7.5$  m), and CHANGES in the stores decreased by  $8$  mm (Q1).

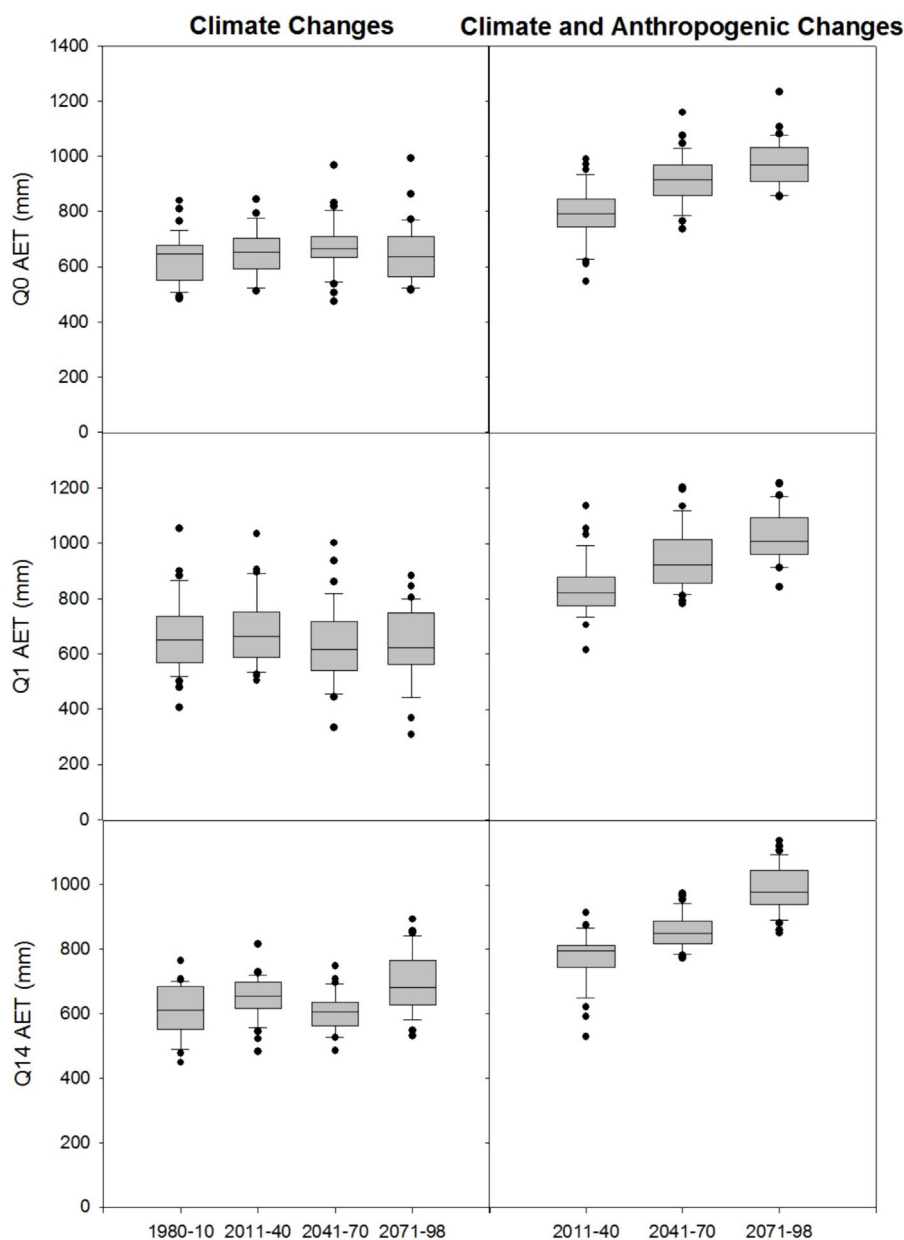


**FIGURE 12** Actual evapotranspiration in all time slices and climate projections. The left column shows changes in AET due to climate change alone, and the right column shows changes in AET due to climate and anthropogenic changes.

## 5 | DISCUSSION

Using historical long-term data, several studies have previously discussed climate change and its impact on catchment hydrology at different time scales. For example, historical data indicated an increase in temperature of approximately  $0.2^{\circ}\text{C}$  from 1950 to 1980 and  $0.7^{\circ}\text{C}$  from 1986 to 2000, which accounted for a decrease in runoff and an increase in actual evapotranspiration in various subcatchments of the basin (Afzal et al., 2020; Afzal & Ragab, 2020b; Bouwer et al., 2006). Similar changes in the future have also been identified by several studies conducted at the regional and Indian subcontinental levels using different climate models. For example, a study at the Indian subcontinent scale predicted an

increase in the average temperature of  $3\text{--}6^{\circ}\text{C}$  by the end of the century (higher temperatures in the north than in the south) (Kumar et al., 1994; Kumar et al., 2004; Lal et al., 1995).

In this study, the potential impacts of future climate and anthropogenic changes on catchment hydrology are examined. For this purpose, the calibrated and validated modified SWAT model is forced with bias-corrected PRE-CIS future climate projection data (Q0, Q1 and Q14) and predicted anthropogenic changes in the catchment. Model results are analysed to assess the individual and combined impacts of climate change and anthropogenic catchment changes on the hydrology of the HS catchment. We simulated two scenarios: first, keeping the observed catchment changes constant before the baseline

(2010) period and changing only the climate, as in all future climate projections. The second scenario estimates the impact of anthropogenic changes occurring in the HS catchment in the future up to 2099.

## 5.1 | Comparison of climate and catchment change impacts

The results indicate that although the mean surface temperature will increase continuously (0.7–2.3 °C) in the future, its impact on SF and AET will be small when the annual rainfall is greater than the average annual rainfall. Compared to the baseline period, the data indicate that the average monthly rainfall will change between –20 and 23% in the future (4 and 9% during the early century, –8 to 23% during the middle century and from –20 to 6% at the end of the century). By the end of the century, it was also observed that the maximum monthly rainfall (i.e. the month with the highest rainfall in a year) shifted from August to September. Lal et al. (2001) and Mall (2006) noted a 5–25% increase in average annual rainfall and greater variability in the onset of the Indian monsoon season by the end of the century.

Considering only the impact of future climate change, it can be observed that the streamflow becomes stronger according to the average annual rainfall (rainfall–runoff ratios changed from 9 to 31%) in the catchment, as shown in Figure 13a. However, when catchment changes are considered along with climate change, the rainfall–runoff ratios decrease drastically between 4 and 12%, as shown in Figure 13b (Afzal & Ragab, 2019). The contribution of base flow to streamflow will likely play a key role in the future. When only climate change was considered, the contribution of base flow to streamflow was significantly greater for both low (20–30%) and high (60–70%) rainfall events. Moreover, the base flow contribution is greater than the surface flow contribution when the annual rainfall exceeds 20% of the base case scenario. However, due to both climate and anthropogenic changes, the base flow contribution to streamflow was found to decrease by –70% and may even approach zero in the future. In the HS catchment, potential evapotranspiration may decrease in the future, as shown in Figures 13c, d. In only the climate change scenario may the actual evapotranspiration (AET) change according to the annual rainfall of that year. However, when catchment changes are included, especially due to an increase in irrigation area of 100 ha in each time slice, AET increases (more than 13% for every time slice) despite higher rainfall in the future. The streamflow into the HS reservoir will also be greatly affected by the combination of climate and catchment changes in the future.

Details of future hydrological changes due to individual and combined climate and anthropogenic influences compared to those in the baseline period are shown in Figure 14. As the irrigated area is predicted to increase in the future, the irrigation requirements are expected to increase in each time slice. The irrigation requirements were found to increase at rates of 3, 5 and 7 times (early century: 195–205 mm; middle century: 366–461 mm; and end century: 437–543 mm) compared to those in the baseline period if the same land use trend continues in the future. This greatly affected groundwater storage, which was reduced by 3, 7 and 10 m in the HS catchment in the early, middle and end centuries, respectively. Due to the increased capacities of water storage structures in the future resulting from the implementation of different government watershed programmes, the impact of these structures on streamflow was found to be negligible in wet rainfall (>1.25% of average annual rainfall) years but slightly greater during dry rainfall (<75% of average annual rainfall) years. It was predicted that these structures help to store excess runoff (3 mm) and control the damage of high flood events, but streamflow into the HS reservoir is reduced by 8 mm during dry rainfall years. The baseflow contribution to the streamflow becomes zero by the end of the early century (2040), which indicates that the irrigated area in the HS catchment should not increase beyond 100 ha in the future. Overall, the model results strongly suggest that these catchment changes will lead to greater stress on both streamflow and groundwater storage during dry and normal rainfall years in the HS catchment in the future, as observed in many other catchments (Figure 14) (Afzal & Ragab, 2020a).

Three overall inferences can be drawn from the above discussion. First, catchment changes are projected to have greater impacts than climate change if the scenarios are considered. Second, the influence of annual rainfall on HS streamflow (decreases) and evapotranspiration (increases) weakens when catchment changes are incorporated into the projections (Figures 13 b, d). Third, in all climate projections (Q0, Q1 and Q14) and in all three time slices, the water balance components are more sensitive to changes in annual rainfall and temporal variability of monthly rainfall than to changes in average annual temperature.

## 5.2 | Uncertainties in climate change projections

It is well known that projections of future emissions contain inherent uncertainties in the assumptions and their relationships to population, socio-economic development and technological changes that underpin the IPCC emission scenarios (Morita et al., 2000). In addition to

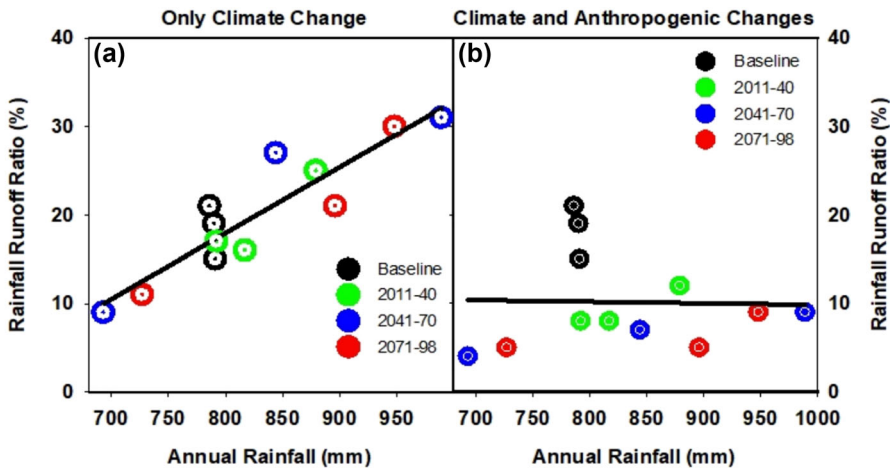


FIGURE 13 Relating the average annual rainfall to streamflow: (a) due to only climate change; (b) due to both climate and anthropogenic changes; to potential and actual evapotranspiration; (c) due to only climate change; and (d) due to both climate and anthropogenic changes.

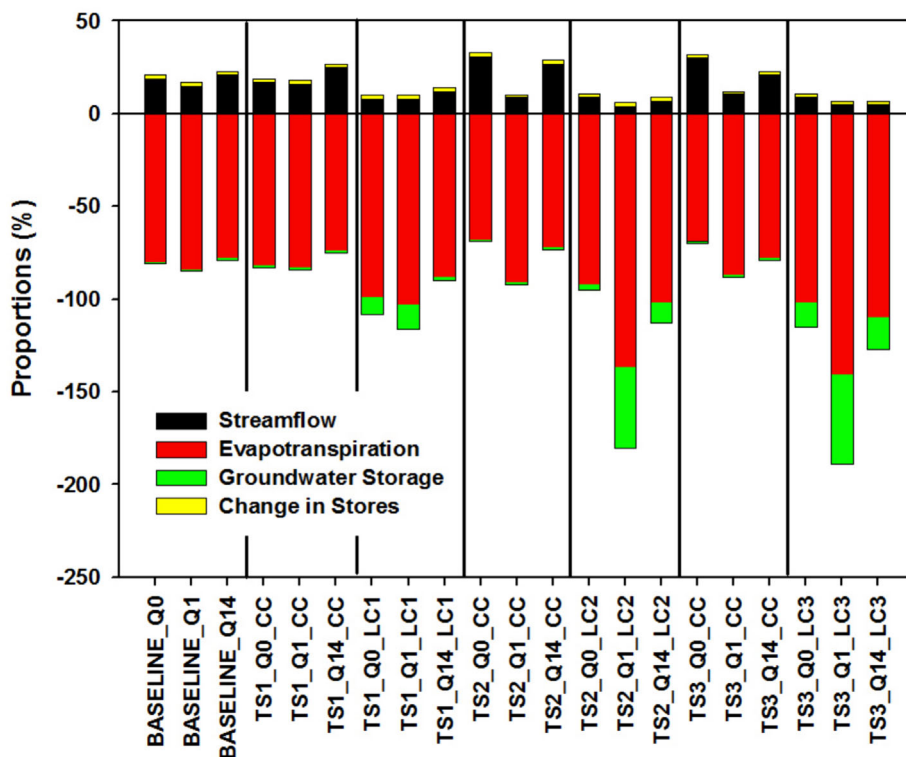
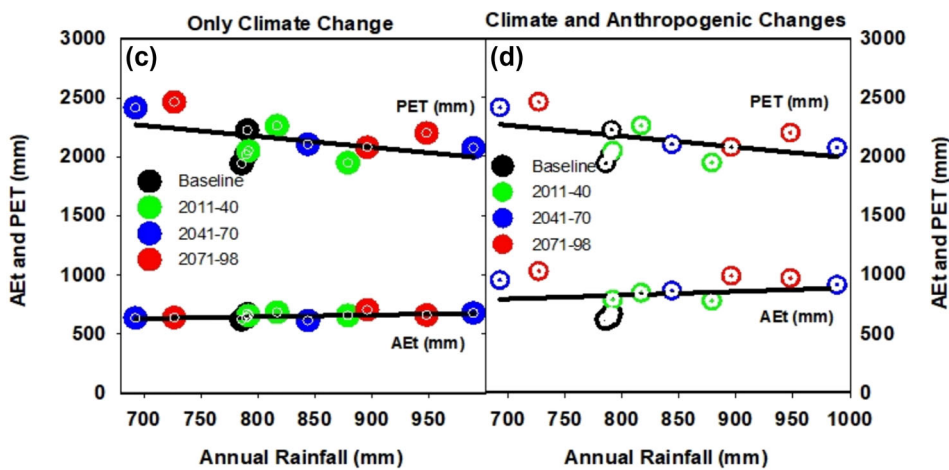


FIGURE 14 Percentage changes from the baseline in streamflow, evapotranspiration and groundwater storage in the Himayat Sagar catchment in the future. TS1/2/3 indicate the near-century/middle-century/end-century periods, respectively, and LC1/2/3 indicate the 100/200/285 km<sup>2</sup> increase in the irrigated area, respectively (along with the other corresponding catchment changes).

uncertainty in future emissions, uncertainties in the conversion of emissions into concentrations by global models are added due to an incomplete understanding of some of the key processes, the physics of the carbon cycle and chemical reactions of the atmosphere (Jones et al., 2004). In addition to the above uncertainties, the atmospheric uncertainty of greenhouse gas concentrations needs to be considered; for example, an increase in the atmospheric concentration of CO<sub>2</sub> from 300 to 600 ppm could increase the surface temperature of the Earth by 5°C, while a decrease in the CO<sub>2</sub> concentration of 150 ppm could lead to surface cooling. Therefore, it can be clearly understood that there is uncertainty in the prediction of climate models due to the representation of internal model dynamics (Afzal & Ragab, 2019; Ragab et al., 2020). Figure 14 clearly shows the uncertainty in future streamflow, actual evapotranspiration and groundwater storage for different climate projections, particularly the Q1 and Q14 simulations in the HS catchment.

## 6 | CONCLUSIONS

The HS catchment underwent many changes over the study period. Therefore, the streamflow decreased, and the groundwater level decreased. This study explored the impact of potential future climate and catchment changes on future hydrological processes in the HS catchment. Future trends in catchment condition changes are assumed to be a moderated version of what they have been over the past three decades. This is particularly likely if current policies on water and water tanks are maintained. Overall, it is clear that both climate and anthropogenic changes are important, and they tend to have opposite influences, given the projections of increased rainfall, water interception and usage, although there are considerable differences in rainfall among the three climate projections. Nevertheless, unless current policies are modified to stabilize land use and water abstraction, anthropogenic change is likely to be more important than climate change (Gosling & Arnell, 2016; Haddeland et al., 2014). Climate change could provide some buffer in the future with increased rainfall. If climate and anthropogenic changes are not modelled properly using a coupled model, inaccurate recommendations for water harvesting and agricultural expansion may occur.

## ETHICAL APPROVAL AND CONSENT TO PARTICIPATE

Not applicable.

## CONSENT TO PUBLISH

All the authors agreed to publish the manuscript.

## AUTHOR CONTRIBUTIONS

**Rajesh Nune:** Data collection; methodology; model development; manuscript draft preparation and scenario development. **Andrew W. Western:** Model development; conceptualization; overall supervision; reviewing; manuscript editing. **Biju A. George:** Manuscript editing; reviewing; data corrections; supervising. **Sridhar Gummadi:** Climate data analysis; manuscript editing. **Srinivas Pasupuleti:** Reviewing manuscript editing; scenario development. **Ragab Ragab:** Manuscript editing; reviewing; model scenario development. **Sreenath Dixit:** Reviewing; manuscript editing.

## ACKNOWLEDGEMENTS

We wish to thank Dr Murray Peal, University of Melbourne, for his kind support during bias correction of the climate data. We also thank Dr Suhas P. Wani for his valuable suggestions during the development of the model scenarios. Thanks are due to all the Indian government departments mentioned in this paper for providing valuable data. The International Water Management Institute (IWMI), ICRISAT and Hyderabad provided office space during fieldwork in India. This research was funded by the Australian Centre for International Agricultural Research (ACIAR) through a John Allwright Fellowship Award to the first author. The Robert Bage Memorial Scholarship from the University of Melbourne funded the first author to conduct fieldwork. Open access publishing facilitated by The University of Melbourne, as part of the Wiley - The University of Melbourne agreement via the Council of Australian University Librarians.

## CONFLICT OF INTEREST STATEMENT

No potential conflicts of interest were reported by the authors.

## DATA AVAILABILITY STATEMENT

Not applicable.

## ORCID

Rajesh Nune  <https://orcid.org/0000-0002-9737-4986>

Ragab Ragab  <https://orcid.org/0000-0003-2887-7616>

## REFERENCES

- Afzal, M. & Ragab, R. (2019) Drought risk under climate and land use changes: implication to water resource availability at catchment scale. *Water*, 11(9), 1790. Available from: <https://doi.org/10.3390/w11091790>

- Afzal, M. & Ragab, R. (2020) Impact of the future climate and land use changes on the hydrology and water resources in south East England, UK. *American Journal of Water Resources.*, 8, 218–231. <https://pubs.sciepub.com/ajwr/8/5/2/index.html>
- Afzal, M. & Ragab, R. (2020a) Assessment of the potential impacts of climate change on the hydrology at catchment scale: modelling approach including prediction of future drought events using drought indices. *Applied Water Science*, 10(10), 215. Available from: <https://doi.org/10.1029/2021WR031347>
- Afzal, M. & Ragab, R. (2020b) How do climate and land use changes affect the water cycle? Modelling Study Including Future Drought Events Prediction Using Reliable Drought Indices. *Irrig. And Drain.*, 69(4), 806–825. Available from: <https://doi.org/10.1002/ird.2467>
- Afzal, M., Vavlas, N. & Ragab, R. (2020) Modelling study to quantify the impact of future climate and land use changes on water resources availability at catchment scale. *Journal of Water and Climate Change*, 12(2), 339–361. Available from: <https://doi.org/10.2166/wcc.2020.117>
- Alemayehu, T., Furi, W. & Legesse, D. (2007) Impact of water over-exploitation on highland lakes of eastern Ethiopia. *Environmental Geology*, 52(1), 147–154. Available from: <https://doi.org/10.1007/s00254-006-0468-x>
- Allen, C.D., Macalady, A.K., Chenchouni, H., Bachelet, D., McDowell, N., Vennetier, M., et al. (2010) A global overview of drought and heat-induced tree mortality reveals emerging climate change risks for forests. *Forest Ecology and Management*, 259(4), 660–684. Available from: <https://doi.org/10.1016/j.foreco.2009.09.001>
- Allen, R.G., Pereira, L.S., Raes, D. & Smith, M. (1998) Crop evapotranspiration - guidelines for computing crop water requirements. In: *Irrigation and drainage, paper no. 56*. Rome, Italy: FAO, p. 300 [https://appgeodb.nancy.inra.fr/biljou/pdf/Allen\\_FAO1998.pdf](https://appgeodb.nancy.inra.fr/biljou/pdf/Allen_FAO1998.pdf)
- Arnold, J.G. & Fohrer, N. (2005) SWAT2000: current capabilities and research opportunities in applied watershed modelling. *Hydrological Processes*, 19(3), 563–572. Available from: <https://doi.org/10.1002/hyp.5611>
- Arnold, J.G., Srinivasan, R., Muttiyah, R.S. & Williams, J.R. (1998) Large area hydrologic modelling and assessment part I: model development. *JAWRA Journal of the American Water Resources Association*, 34(1), 73–89. Available from: <https://doi.org/10.1111/j.1752-1688.1998.tb05961.x>
- Ashraf, M., Kahlowan, M.A. & Ashfaq, A. (2007) Impact of small dams on agriculture and groundwater development: A case study from Pakistan. *Agricultural Water Management*, 92(1-2), 90–98. Available from: <https://doi.org/10.1016/j.agwat.2007.05.007>
- Baloch, M., Ames, D. & Tanik, A. (2015) Hydrologic impacts of climate and land-use change on Namnam stream in Koycegiz watershed, Turkey. *International Journal of Environmental Science & Technology (IJEST)*, 12(5), 1481–1494. Available from: <https://doi.org/10.1007/s13762-014-0527-x>
- Beavis, S.G., Zhang, L., Evans, J.P., Jakeman, A. & Smith, D.L. (1997) impacts and implications of farm dams on catchment hydrology: methods and application to Chafrey catchment. In: *MODSIM 97 - IMACS*. Australia: The Modelling and Simulation Society of Australia Inc. <https://www.mssanz.org.au/MODSIM97/Vol%201/Beavis2.pdf>
- Bouwer, L.M., Aerts, J.C.J.H., Droogers, P. & Dolman, A.J. (2006) Detecting the long-term impacts from climate variability and increasing water consumption on runoff in the Krishna River basin (India). *Hydrology and Earth System Sciences*, 10(5), 703–713. Available from: <https://doi.org/10.5194/hess-10-703-2006>
- Callow, J.N. & Smettem, K.R.J. (2009) The effect of farm dams and constructed banks on hydrologic connectivity and runoff estimation in agricultural landscapes. *Environmental Modelling and Software*, 24(8), 959–968. Available from: <https://doi.org/10.1016/j.envsoft.2009.02.003>
- Chiew, F.H.S. & McMahon, T.A. (2002) Modelling the impacts of climate change on Australian streamflow. *Hydrological Processes*, 16(6), 1235–1245. Available from: <https://doi.org/10.1002/hyp.1059>
- Cooley, S.W., Ryan, J.C. & Smith, L.C. (2021) Human alteration of global surface water storage variability. *Nature*, 591(7848), 78–81. Available from: <https://doi.org/10.1038/s41586-021-03262-3>
- Cristea, N.C. & Burges, S.J. (2010) An assessment of the current and future thermal regimes of three streams located in the Wenatchee River basin, Washington State: some Implications for Regional River Basin Systems. *Climatic Change*, 102(3-4), 493–520. Available from: <https://doi.org/10.1007/s10584-009-9700-5>
- Desai, S., Singh, D.K., Islam, A. & Sarangi, A. (2020) Impact of climate change on the hydrology of a semiarid river basin of India under hypothetical and projected climate change scenarios. *Journal of Water and Climate Change*, 12(3), 969–996. Available from: <https://doi.org/10.2166/wcc.2020.287>
- Dewandel, B., Lachassagne, P., Wyns, R., Maréchal, J.C. & Krishnamurthy, N.S. (2006) A generalized 3-D geological and hydrogeological conceptual model of granite aquifers controlled by single or multiphase weathering. *Journal of Hydrology*, 330(1-2), 260–284. Available from: <https://doi.org/10.1016/j.jhydrol.2006.03.026>
- Dingbao, W. & Alimohammadi, N. (2012) Responses of annual runoff, evaporation, and storage change to climate variability at the watershed scale. *Water Resources Research*, 48, 1–16. Available from: <https://doi.org/10.1029/2011WR011444>
- Ficklin, D.L., Stewart, I.T. & Maurer, E.P. (2013) Effects of projected climate change on the hydrology in the mono Lake basin, California. *Climatic Change*, 116(1), 111–131. Available from: <https://doi.org/10.1007/s10584-012-0566-6>
- Garg, K.K., Karlberg, L., Barron, J., Wani, S.P. & Rockstrom, J. (2012) Assessing impacts of agricultural water interventions in the Kothapally watershed, South India. *Hydrological Processes*, 26(3), 387–404. Available from: <https://doi.org/10.1002/hyp.8138>
- George, B., Malano, M. H. & Davidson, B. (2007) Integrated water allocation-economic modelling at a catchment scale. In: *MODSIM-2007*, [https://www.mssanz.org.au/MODSIM07/papers/5\\_s45/IntigratedWater\\_s45\\_George.pdf](https://www.mssanz.org.au/MODSIM07/papers/5_s45/IntigratedWater_s45_George.pdf)
- Gordon, C., Cooper, C., Senior, C.A., Banks, H., Gregory, J.M., Johns, T.C., et al. (2000) The simulation of SST, sea ice extents and ocean heat transports in a version of the Hadley Centre coupled model without flux adjustments. *Climate Dynamics*, 16(2-3), 147–168. Available from: <https://doi.org/10.1007/s003820050010>
- Gosain, A.K., Rao, S. & Basuray, D. (2006) Climate change impact assessment on hydrology of Indian River basins. *Current Science*, 90, 346–353. <https://www.jstor.org/stable/24091868>
- Gosling, S.N. & Arnell, N.W. (2016) A global assessment of the impact of climate change on water scarcity. *Climatic Change*,



- 134(3), 371–385. Available from: <https://doi.org/10.1007/s10584-013-0853-x>
- Gumma, M.K., Panjala, P., Deevi, K.C., Bellam, P.K., Dheeravath, V. & Mohammed, I. (2023) Impacts of irrigation tank restoration on water bodies and croplands in Telangana state of India using Landsat time series data and machine learning algorithms. *Geocarto International*, 38(1), 2186493. Available from: <https://doi.org/10.1080/10106049.2023.2186493>
- Gurunadha Rao, V.V.S., Suryanarayana, G., Prakash, B.A., Mahesh Kumar, K. & Ramesh, M. (2007) Ecological study of Osmansagar and Himayatsagar lakes in greater Hyderabad, Andhra Pradesh, India. *Environmental Sciences*. <https://api.semanticscholar.org/CorpusID:130022384>
- Haddeland, I., Heinke, J., Biemans, H., Eisner, S., Florke, M., Hanasaki, N., et al. (2014) Global water resources affected by human interventions and climate change. *Proceedings of the National Academy of Sciences of the United States of America*, 111(9), 3251–3256. Available from: <https://doi.org/10.1073/pnas.1222475110>
- IPCC. (2007) *Climate change 2007: synthesis report. Contribution of working groups I, II and III to the fourth assessment report of the intergovernmental panel on climate change [Core writing team, Pachauri, R. K and Reisinger, A. (eds.)]*. Geneva, Switzerland: IPCC 104 pp. <https://www.ipcc.ch/report/ar4/syr/>
- IPCC. (2014) *Climate change 2014: synthesis report. In: contribution of working groups I, II and II to the fifth assessment report of the intergovernmental panel on climate change, [Core writing team, R.K. Pachauri and L.A. Meyer (eds.)]*. Geneva, Switzerland: IPCC, p. 151 pp. <https://www.ipcc.ch/report/ar5/syr/>
- IPCC, 2023: *Summary for policymakers. In: climate change 2023: synthesis report. Contribution of working groups I, II and III to the sixth assessment report of the intergovernmental panel on climate change [Core writing team, H. Lee and J. Romero (eds.)]*. IPCC, Geneva, Switzerland, pp. 1–34, doi: <https://doi.org/10.59327/IPCC/AR6-9789291691647>. [https://www.ipcc.ch/report/ar6/syr/downloads/report/IPCC\\_AR6\\_SYR\\_Longer\\_Report.pdf](https://www.ipcc.ch/report/ar6/syr/downloads/report/IPCC_AR6_SYR_Longer_Report.pdf)
- Jayatilaka, C., Sakthivadivel, R., Shinogi, Y., Makin, I.W. & Witharana, P.J. (2003) A simple water balance modelling approach for determining water availability in an irrigation tank cascade system. *Journal of Hydrology*, 273(1–4), 81–102. Available from: [https://doi.org/10.1016/S0022-1694\(02\)00360-8](https://doi.org/10.1016/S0022-1694(02)00360-8)
- Jones, R.G., Noguer, M., Hassell, D.C., Hudson, D., Wilson, S.S., Jenkins, G.J., et al. (2004) *Generating high resolution climate change scenarios using PRECIS*. Exeter, UK: Met Office Hadley Centre, p. 40 pp. [https://www.metoffice.gov.uk/binaries/content/assets/metofficegovuk/pdf/research/applied-science/precis/precis\\_handbook.pdf](https://www.metoffice.gov.uk/binaries/content/assets/metofficegovuk/pdf/research/applied-science/precis/precis_handbook.pdf)
- Jordan, P.W., Wiesenfeld, C.R., Hill, P.I., Morden, R.A. & Chiew, F.H.S. (2008) *An assessment of the future impact of farm dams on runoff in the Murray-Darling basin, Australia*. Australia: Engineers Australia. <https://api.semanticscholar.org/CorpusID:129986441>
- Kumar, K.R.K., Krishna, K. & Pant, G.B. (1994) Diurnal asymmetry of surface temperature trends over India. *Geophysical Research Letters*, 21, 677–680. Available from: <https://doi.org/10.1029/94GL00007>
- Kumar, K.K., Kumar, K.R., Ashrit, R.G., Deshpande, N.R. & Hansen, J.W. (2004) Climate impacts on Indian agriculture. *International Journal of Climatology*, 24(11), 1375–1393. Available from: <https://doi.org/10.1002/joc.1081>
- Kumar, K.K., Patwardhan, S.K., Kulkarni, A., Kamala, K., Rao, K.K. & Jones, R. (2011) Simulated projections for summer monsoon climate over India by a high-resolution regional climate model (PRECIS). *Current Science*, 101, 312–326. <https://www.currentscience.ac.in/Volumes/101/03/0312.pdf>
- Kundzewicz, Z.W. & Robson, A.J. (2004) Change detection in hydrological records - a review of the methodology/Revue méthodologique de la détection de changements dans les chroniques hydrologiques. *Hydrological Sciences Journal*, 49(1), 7–19. Available from: <https://doi.org/10.1623/hysj.49.1.7.53993>
- Kusangaya, S., Warburton, M.L., Archer van Garderen, E. & Jewitt, G.P.W. (2014) Impacts of climate change on water resources in southern Africa. *A review. of the Earth Physics and Chemistry*, 67–69, 47–54. Available from: <https://doi.org/10.1016/j.pce.2013.09.014>
- Lal, M., Cubasch, U., Voss, R. & Waszkewitz, J. (1995) Effect of transient increase in greenhouse gases and sulphate aerosols on monsoon climate. *Current Science*, 69, 752–763. <https://www.currentscience.ac.in/Volumes/69/09/0752.pdf>
- Lal, M., Nozawa, T., Emori, S., Harasawa, H., Takahashi, K., Kimoto, M., et al. (2001) Future climate change: implications for Indian summer monsoon and its variability. *Current Science*, 81, 1196–1207. <https://www.currentscience.ac.in/Volumes/81/09/1196.pdf>
- Mall, R.K., Singh, R., Gupta, A., Srinivasan, G. & Rathore, L.S. (2006) Impact of climate change on Indian agriculture: A review. *Climatic Change*, 78(2–4), 445–478. Available from: <https://doi.org/10.1007/s10584-006-9236-x.pdf>
- Marvel, K., Cook, B.I., Bonfils, C.J.W., Durack, P.J., Smerdon, J.E. & Williams, A.P. (2019) Twentieth-century hydroclimate changes consistent with human influence. *Nature*, 569(7754), 59–65. Available from: <https://doi.org/10.1038/s41586-019-1149-8>
- Massuel, S., George, B., Venot, J.P., Bharati, L. & Acharya, S. (2013) Improving assessment of groundwater-resource sustainability with deterministic modelling: A case study of the semiarid Musi subbasin, South India. Mejora de la evaluación de la sustentabilidad del recurso de agua subterránea con un modelado determinístico: un Caso de estudio de la subcuenca semiárida de Musi, Sur de India. *Hydrogeology Journal*, 21, 1567–1580. Available from: <https://doi.org/10.1007/s10040-013-1030-z>
- Middelkoop, H., Daamen, K., Gellens, D., Grabs, W., Kwadijk, J.C.J., Lang, H., et al. (2001) Impact of climate change on hydrological regimes and water resources management in the Rhine basin. *Climatic Change*, 49, 105–128. Available from: <https://doi.org/10.1023/A:1010784727448>
- Mittal, N., Bhave, A.G., Mishra, A. & Singh, R. (2016) Impact of human intervention and climate change on natural flow regime. *Water Resources Management*, 30(2), 685–699. Available from: <https://doi.org/10.1007/s11269-015-1185-6>
- Mohammed, A.K., Hirmas, D.R., Nemes, A. & Giménez, D. (2020) Exogenous and endogenous controls on the development of soil structure. *Geoderma*, 357, 113945. Available from: <https://doi.org/10.1016/j.geoderma.2019.113945>
- Morita, T., Nakićenović, N. & Robinson, J. (2000) Overview of mitigation scenarios for global climate stabilization based on new IPCC emission scenarios (SRES). *Environmental Economics and*

- Policy Studies*, 3(2), 65–88. Available from: <https://doi.org/10.1007/BF03354031>
- Müller, M.F. & Levy, M.C. (2019) Complementary vantage points: integrating hydrology and economics for sociohydrologic knowledge generation. 55, 2549–2571. Available from: <https://doi.org/10.1029/2019WR024786>
- Murugan, M., Shetty, P.K. & Hiremath, M.B. (2005) Atmospheric warming induced changes in future rainfall and implications on water and agriculture in India. *Caspian Journal of Environmental Science*, 3, 132–141. [https://cjes.guilan.ac.ir/article\\_972.html](https://cjes.guilan.ac.ir/article_972.html)
- Nash, J.E. & Sutcliffe, J.V. (1970) River flow forecasting through conceptual models part I - A discussion of principles. *Journal of Hydrology*, 10(3), 282–290. Available from: [https://doi.org/10.1016/0022-1694\(70\)90255-6](https://doi.org/10.1016/0022-1694(70)90255-6)
- Neal, B., Nathan, R.J., Schreider, S. & Jakeman, A.J. (2002) Identifying the separate impact of farm dams and land use changes on catchment yield. *Australasian Journal of Water Resources*, 5(2), 165–176. Available from: <https://doi.org/10.1080/13241583.2002.11465202>
- Neitsch, S.L., Arnold, J.G., Kiniry, J.R. & Williams, J.R. (2009) In: SaWRL, G. (Ed.) *Soil and water Assessment tool theoretical documentation version 2009*. <https://swat.tamu.edu/media/99192/swat2009-theory.pdf>
- Niehoff, D., Fritsch, U. & Bronstert, A. (2002) Land use impacts on storm-runoff generation: scenarios of land use change and simulation of hydrological response in a meso-scale catchment in SW-Germany. *Journal of Hydrology*, 267(1-2), 80–93. Available from: [https://doi.org/10.1016/S0022-1694\(02\)00142-7](https://doi.org/10.1016/S0022-1694(02)00142-7)
- Nune, R., George, B., Teluguntla, P. & Western, A. (2014) Relating trends in streamflow to anthropogenic influences: A case study of Himayat Sagar catchment, India. *Water Resources Management*, 28(6), 1579–1595. Available from: <https://doi.org/10.1007/s11269-014-0567-5>
- Nune, R., George, B.A., Western, A.W., Garg, K.K., Dixit, S. & Ragab, R. (2021) A comprehensive assessment framework for attributing trends in streamflow and groundwater storage to climatic and anthropogenic changes: A case study in the typical semiarid catchments of southern India. *Hydrological Processes*, 35(8), e14305. Available from: <https://doi.org/10.1002/hyp.14305>
- Ozkul, S. (2009) Assessment of climate change effects in Aegean River basins: the case of Gediz and Buyuk Menderes basins. *Climatic Change*, 97(1-2), 253–283. Available from: <https://doi.org/10.1007/s10584-009-9589-z>
- Padowski, J.C., Gorelick, S.M., Thompson, B.H., Rozelle, S. & Fendorf, S. (2015) Assessment of human–natural system characteristics influencing global freshwater supply vulnerability. *Environmental Research Letters*, 10, 104014. Available from: <https://doi.org/10.1088/1748-9326/10/10/104014>
- Perkins, S.P. & Sophocleous, M.A. (2000) Combining SWAT and MODFLOW Into an Integrated Watershed Model. In: *Open-File Report No. 2000–67*. Lawrence KS 66047: Kansas Geological Survey, The University of Kansas.
- Perrin, J., Ferrant, S., Massuel, S., Dewandel, B., Maréchal, J.C., Aulong, S., et al. (2012) Assessing water availability in a semi-arid watershed of southern India using a semidistributed model. *Journal of Hydrology*, 460-461, 143–155. Available from: <https://doi.org/10.1016/j.jhydrol.2012.07.002>
- Pohle, I., Koch, H., Conradt, T., Gädeke, A. & Grünwald, U. (2015) Potential impacts of climate change and regional anthropogenic activities in central European mesoscale catchments. *Hydrological Sciences Journal/Journal Des Sciences Hydrologiques*, 60, 912–928. Available from: <https://doi.org/10.1080/02626667.2014.968571>
- Pope, V.D., Gallani, M.L., Rowntree, P.R. & Stratton, R.A. (2000) The impact of new physical parametrizations in the Hadley Centre climate model: HadAM3. *Climate Dynamics*, 16(2-3), 123–146. Available from: <https://doi.org/10.1007/s003820050009>
- Quilbé, R., Rousseau, A.N., Moquet, J.-S., Savary, S., Ricard, S. & Garbouj, M.S. (2008) Hydrological responses of a watershed to historical land use evolution and future land use scenarios under climate change conditions. *Hydrology and Earth System Sciences*, 12(1), 101–110. Available from: <https://doi.org/10.5194/hess-12-101-2008>
- Ragab, R., Kaelin, A., Afzal, M. & Panagea, I. (2020) Application of generalized likelihood uncertainty estimation (GLUE) at different temporal scales to reduce the uncertainty level in modelled river flows. *Hydrological Sciences Journal*, 65(11), 1856–1871. Available from: <https://doi.org/10.1080/02626667.2020.1764961>
- Rajeevan, M., Jyoti, B., Kale, J.D. & Lal, B. (2006) High resolution daily gridded rainfall data for the Indian region: analysis of break and active monsoon spells. *Current Science*, 91, 296–306. <https://www.jstor.org/stable/i24094114>
- Ramabrahmam, K., Keesara, V.R., Srinivasan, R., Pratap, D. & Sridhar, V.J.S. (2021) Flow simulation and storage assessment in an ungauged irrigation tank cascade system using the SWAT model. *Sustainability*, 13(23), 13158. Available from: <https://doi.org/10.3390/su132313158>
- Ribeiro, C.L.C., Diotto, A.V., Thebaldi, M.S., Rodrigues, J.A.M. & Viola, M.R. (2022) Simulations of the climate change and its effect on water resources in the Palma River basin, Brazil. *Water Supply*, 22(5), 5494–5508. Available from: <https://doi.org/10.2166/ws.2022.184>
- Rockstrom, J., Falkenmark, M., Karlberg, L., Hoff, H., Rost, S. & Gerten, D. (2009) Future water availability for global food production: the potential of green water for increasing resilience to global change. *Water Resources Research*, 45(7), 1–16. Available from: <https://doi.org/10.1029/2007WR006767>
- Rupa Kumar, K., Sahai, A.K., Krishna Kumar, K., Patwardhan, S.K., Mishra, P.K., Revadekar, J.V., et al. (2006) High-resolution climate change scenarios for India for the 21st century. *Current Science*, 90, 334–345. <http://www.jstor.org/stable/24091867>
- Saft, M., Western, A.W., Zhang, L., Peel, M.C. & Potter, N.J. (2015) The influence of multiyear drought on the annual rainfall-runoff relationship: an Australian perspective. *Water Resources Research*, 51(4), 2444–2463. Available from: <https://doi.org/10.1002/2014WR015348>
- Schreider, S.Y., Jakeman, A.J., Letcher, R.A., Nathan, R.J., Neal, B.P. & Beavis, S.G. (2002) Detecting changes in streamflow response to changes in nonclimatic catchment conditions: farm dam development in the Murray-Darling basin, Australia. *Journal of Hydrology*, 262(1-4), 84–98. Available from: [https://doi.org/10.1016/S0022-1694\(02\)00023-9](https://doi.org/10.1016/S0022-1694(02)00023-9)
- Senent-Aparicio, J., Liu, S., Pérez-Sánchez, J., López-Ballesteros, A. & Jimeno-Sáez, P. (2018) Assessing impacts of climate variability and reforestation activities on water resources in the headwaters of the Segura River basin

- (SE Spain). *Sustainability*, 10(9), 3277. Available from: <https://doi.org/10.3390/su10093277>
- Shiklomanov, I.A. (1989) Climate and water resources. *Hydrological Sciences Journal*, 34(5), 495–529. Available from: <https://doi.org/10.1080/02626668909491359>
- Shiklomanov, I. A. (1997) Comprehensive assessment of the freshwater resources of the world. In: Institute WaSE. (Ed.). <https://www.ircwash.org/resources/comprehensive-assessment-freshwater-resources-world>
- Shiklomanov, I.A., Babkin, V.I. & Balonishnikov, Z.A. (2011) Water resources, their use, and water availability in Russia: current estimates and forecasts. *Water Resources*, 38(2), 139–148. Available from: <https://doi.org/10.1134/S009780781101012X>
- Siriwardena, L., Finlayson, B.L. & McMahon, T.A. (2006) The impact of land use change on catchment hydrology in large catchments: the Comet River, Central Queensland, Australia. *Journal of Hydrology*, 326(1-4), 199–214. Available from: <https://doi.org/10.1016/j.jhydrol.2005.10.030>
- Stone, D.A. & Hansen, G. (2016) Rapid systematic assessment of the detection and attribution of regional anthropogenic climate change. *Climate Dynamics*, 47(5-6), 1399–1415. Available from: <https://doi.org/10.1007/s00382-015-2909-2>
- The MathWorks Inc. 2012. Optimization Toolbox version: 9.4 (R2012b). [https://www.mathworks.com/products.html?s\\_tid=gn\\_ps](https://www.mathworks.com/products.html?s_tid=gn_ps)
- Thiemeßl, M., Gobiet, A. & Heinrich, G. (2012) Empirical-statistical downscaling and error correction of regional climate models and its impact on the climate change signal. *Climatic Change*, 112(2), 449–468. Available from: <https://doi.org/10.1007/s10584-011-0224-4>
- Venkateswara Rao, B., Nune, R., Rajesh, M.V.S. & Vijaya Sarada, S.T. (2006) Large scale groundwater withdrawal and closing basin - A case study of the upper Musi basin, India. *International Journal of Water*, 6(2), 15–28. Available from: <https://doi.org/10.1134/S009780781101012X>
- Water Technology Centre. (2008) *Andhra Pradesh soils profile characteristics handbook*. Telangana State, India: Professor Jayashankar Telangana State Agricultural University.
- Yang, D., Yang, Y. & Xia, J. (2021) Hydrological cycle and water resources in a changing world: A review. *Geography and Sustainability*, 2(2), 115–122. Available from: <https://doi.org/10.1016/j.geosus.2021.05.003>
- Zhang, S. & Lu, X.X. (2009) Hydrological responses to precipitation variation and diverse human activities in a mountainous tributary of the lower Xijiang, China. *Catena*, 77(2), 130–142. Available from: <https://doi.org/10.1016/j.catena.2008.09.001>
- Zhang, K., Ruben, G.B., Li, X., Li, Z., Yu, Z., Xia, J., et al. (2020) A comprehensive assessment framework for quantifying climatic and anthropogenic contributions to streamflow changes: A case study in a typical semiarid North China basin. *Environmental Modelling and Software*, 128, 104704. Available from: <https://doi.org/10.1016/j.envsoft.2020.104704>

**How to cite this article:** Nune, R., Western, A.W., George, B.A., Gummadi, S., Pasupuleti, S., Ragab, R. et al. (2024) An assessment of future climatic and anthropogenic impacts on the hydrological system of a semi-arid catchment. *Irrigation and Drainage*, 1–27. Available from: <https://doi.org/10.1002/ird.3018>